npj | precision oncology

Article

Published in partnership with The Hormel Institute, University of Minnesota

https://doi.org/10.1038/s41698-025-00949-y

# HDAC6 facilitates LUAD progression by inducing EMT and enhancing macrophage polarization towards the M2 phenotype



Yantao Jiang[1,4], Ju Zhang[2,4], Junjie Yu[1,4], Wei Luo[1], Qingwu Du[1], Wenting Liu[3], Qi Xu[1], Xueyang Li[1], Huiyan Liu[1], Dingzhi Huang[1] ✉ & Tingting Qin[1] ✉

Histone deacetylase 6 (HDAC6) plays a critical role in lung adenocarcinoma (LUAD) prognosis and the tumor immune microenvironment (TIME). This study, utilizing public datasets and experimental validation, revealed that HDAC6 is upregulated in LUAD, correlating with poor survival outcomes and an immunosuppressive TIME characterized by increased Tregs, CAFs, M2 macrophages, and MDSCs. HDAC6-high patients showed reduced immunotherapy response. HDAC6 knockout inhibited tumor growth, suppressed PI3K/AKT/mTOR signaling and EMT, and enhanced apoptosis and M1 macrophage recruitment. HDAC6 inhibition synergized with anti-PD-1 therapy, suggesting a potential combinatorial strategy for LUAD treatment. HDAC6 serves as a key prognostic marker and therapeutic target in LUAD.

Lung cancer is the second most prevalent cancer globally, accounting for approximately 1.8 million deaths each year[1]. And LUAD is the most frequent histological subtype, comprising nearly 40% of all lung cancer patients[2]. Despite the fact that a variety of treatments such as surgery, chemotherapy, targeted therapy, and immunotherapy have become advanced in recent years, the prognosis for LUAD patients is still unsatisfactory[3]. Resistance to targeted and chemotherapeutic agents remains a major problem, and only a small percentage of patients are sensitive to immunotherapy[4]. Overall, the 5-year OS of patients with LUAD remains poor. Therefore, the identification of potential molecular targets and their mechanisms is essential to explore more precise diagnosis and treatment.

Epigenetic silencing has emerged as a significant contributor to the suboptimal effectiveness of current therapeutic strategies in LUAD[5]. Histone acetylation, a vital epigenetic modification, holds a crucial position in regulating tumorigenesis and its progression[1]. This complex process is finely tuned through the dual regulation of histone acetyltransferases (HATs) and histone deacetylases (HDACs), which manipulate gene transcription by attaching or detaching acetyl groups to histones, thereby inducing chromatin remodeling[6]. Prior research has revealed that HDACs are abnormally overexpressed in several cancer types, functioning as oncogenes[7]. Consequently, HDAC inhibitors (HDACis) have been developed as innovative therapeutic agents in cancer treatment, designed to impede tumor progression, curb cell proliferation, diminish angiogenesis, and regulate the infiltration of immune cells within the TIME[8].

HDACs are categorized into two primary classes: zinc-dependent HDACs (Class I, Class II, and Class IV) and NAD-dependent sirtuins (Class III), encompassing a total of 18 subtypes[9]. Among these, HDAC6 stands out structurally and functionally, serving as the sole enzyme in the HDAC family that boasts two catalytic domains (CDs) and a zinc finger ubiquitin-binding domain (Zf-UBD)[10]. HDAC6 exhibits a broad substrate specificity, capable of deacetylating not only histones but also various substrates like HSP90 and α-tubulin, thereby regulating chaperone activities and microtubule dynamics[11]. Notably, HDAC6 is overexpressed in breast, renal, lung, and endometrial cancers, with its upregulation strongly correlated with poor overall survival in these malignancies[12–15]. Furthermore, HDAC6 is implicated in diverse cancer signaling pathways, including the extracellular signal-regulated kinase (ERK) pathway, TGF-β-mediated epithelial-mesenchymal transition (EMT), and the Notch1 signaling pathway[12,16,17]. One study has demonstrated that the combined action of HDAC6 and USP10 enhances cisplatin resistance in lung cancer[18]. However, a comprehensive analysis of the impact of HDAC6 on the survival and prognosis of LUAD patients, the tumor immune microenvironment, and the underlying regulatory mechanisms remains elusive.

Therefore, to address the aforementioned questions, this study conducted an exhaustive investigation into the associations between HDAC6

[1]Department of Thoracic Oncology, Tianjin Medical University Cancer Institute and Hospital, National Clinical Research Center for Cancer, Tianjin Key Laboratory of Cancer Prevention and Therapy, Tianjin's Clinical Research Center for Cancer, Tianjin, China. [2]Department of Nuclear Medicine, Rizhao People's Hospital, Rizhao, China. [3]Department of Respiratory Medicine, Beijing Friendship Hospital, Capital Medical University, Beijing, China. [4]These authors contributed equally: Yantao Jiang, Ju Zhang, Junjie Yu.
✉e-mail: huangdingzhi@tjmuch.com; qintingting@tjmuch.com

expression and various factors such as prognosis, immune cell infiltration, and macrophage polarization in LUAD patients, utilizing tumor-related databases including The Cancer Genome Atlas (TCGA), Gene Expression Omnibus (GEO), and Clinical Proteomic Tumor Analysis Consortium (CPTAC). Our findings revealed that LUAD patients exhibiting high HDAC6 expression were characterized by poorer survival outcomes and an immunosuppressive tumor microenvironment. Furthermore, we employed clinical data to validate the prognostic significance of HDAC6 in LUAD and its influence on macrophage polarization, aiming to contribute insights that could inform precision treatment strategies for LUAD.

## Results

### Expression landscape of HDAC6 gene in pan-cancer and LUAD

Utilizing the TCGA database, we observed a significant upregulation of HDAC6 in 13 types of tumors, including LUAD (Fig. 1A). Further exploration through the HPA database revealed that HDAC6 localization in cells of various cancer types, such as Rh30 (rhabdomyosarcoma cells), Hela (cervical cancer cells), and U2OS (primary osteosarcoma cells), exhibited both cytoplasmic and nuclear distribution, with a predominant cytoplasmic localization in some cells (Fig. 1B). Additionally, we demonstrated that HDAC6 mRNA levels were significantly elevated in LUAD tumor tissues compared to normal lung tissues using both the CPTAC and GEO databases (including datasets GES27262, GSE75027, GES19188, GES68465, and GSE31210) (Fig. 1C–E). Our analyses with the TCGA and CPTAC databases also showed that HDAC6 protein abundance was significantly higher in patients with LUAD compared to normal lung tissue (Fig. 1F). Furthermore, there was a significant positive correlation between protein and mRNA levels ($R = 0.6102$, $P < 0.05$) (Fig. 1G). IHC images sourced from the HPA database indicated that HDAC6 was more highly expressed in lung cancer tissues and primarily localized in the cytoplasm (Fig. 1H). Lastly, the phosphorylation of HDAC6 at the S30 ($P = 0.0008$), S36 ($P < 0.0001$), and S57 ($P = 0.0008$) sites was significantly increased in LUAD compared to adjacent normal tissues (Fig. 2A). Both phosphorylated and total HDAC6 protein levels were higher in LUAD (Fig. 2B).

### Prognostic value of HDAC6 and associations with clinicopathological characteristics in LUAD

As illustrated in Fig. 2C, D, the TCGA database indicated that LUAD patients with high HDAC6 expression exhibited a worse Disease-free Interval (DFI) ($P = 0.0086$) and a trend towards a worse Progression-free Interval (PFI), albeit not reaching statistical significance ($P = 0.19$). Furthermore, the expression of HDAC6 in LUAD was found to correlate with various clinicopathological characteristics. Specifically, Fig. 2E depicted the associations between HDAC6 expression and factors such as age, gender, smoking history, tumor stage, and overall survival time for LUAD patients in the GSE50081 dataset. Our data revealed that high HDAC6 expression was significantly associated with larger tumor size ($P = 0.01$), lymph node involvement ($P = 0.012$), and advanced TNM stage ($P = 0.013$) within the GSE50081 dataset (Fig. 2F–H). Poorly differentiated tumors demonstrated high HDAC6 expression in the GSE68465 dataset (Fig. 2I). Regarding the relationship between expression and survival prognosis, our data analyses suggested that high HDAC6 expression was accompanied by a worse OS in the GSE50081 dataset ($P = 0.012$), a trend towards a worse Disease-Free Survival (DFS) ($P = 0.052$), and a worse PFS in the GSE68465 dataset ($P = 0.033$) (Fig. 2J–L). Collectively, these findings imply that more malignant LUAD tumors, characterized by advanced TNM stage and poor differentiation, exhibit higher HDAC6 expression.

### Differentially expressed genes of HDAC6 by functional enrichment analysis

To elucidate the potential roles of HDAC6 in LUAD, we conducted an exhaustive analysis of the signaling pathways and biological functions associated with HDAC6 co-expressed genes in this disease. Initially, we screened for HDAC6-related differentially expressed genes using stringent criteria ($|\text{Log2FC}| > 2$ and $P < 0.05$), and the results are visually represented in a volcano plot in Fig. 3A. We further highlighted the top 50 upregulated and top 50 downregulated genes with the most significant differential changes through a heatmap (Fig. 3B). The outermost and innermost circles of the heatmap respectively depict the samples categorized into "HDAC6 high expression" and "HDAC6 low expression" groups. KEGG pathway enrichment analysis revealed that HDAC6-associated genes were significantly enriched in pathways such as Neuroactive ligand-receptor interaction, PI3K-AKT signaling, MAPK signaling, Chemokine signaling, and mTOR signaling pathway (all $P < 0.05$) (Fig. 3C). Our GO analysis uncovered that HDAC6-related genes were predominantly enriched in the regulation of signaling and immune system processes (Biological process, BP). Additionally, Molecular functions (MF) were enriched in anion binding, small molecule binding, and drug binding, while the cellular components (CC) most relevant to HDAC6 were identified as integral components of the membrane and cytosol (Fig. 3D). Moreover, our findings revealed that the top three enriched pathways associated with HDAC6 co-expressed genes in the TCGA database, as analyzed on the GSCA website, were PI3K-AKT signaling (FDR = 0.003), mTOR signaling (FDR = 0.0041), and Apoptosis pathway (FDR = 0.03). GSEA enrichment analyses further identified that the top three pathways linked with HDAC6 upregulated genes were enriched in the WNT pathway, JAK-STAT pathway, and PGF pathway (Fig. 3H). Subsequently, the Protein-Protein Interaction (PPI) network demonstrated that the proteins that significantly interacted with HDAC6 primarily functioned in cell proliferation, signal transduction, metabolic regulation, and immune response. Among these, FMOD, MAT1, KLHDC4, and PILRB were the top four proteins that exhibited the most significant interactions with HDAC6 (Fig. 3I).

Additionally, we conducted the aforementioned enrichment analyses on HDAC6-related differential genes using two datasets, GSE50081 and GSE68465, with the results presented in supplementary Fig. 1A–D. Our findings indicated that the functional pathways enriched in both datasets were predominantly focused on tumor proliferation and metastasis-related pathways, such as PI3K-AKT signaling and mTOR signaling pathway. Notably, several immune-related pathways were also enriched, including the T cell receptor signaling pathway and PD-L1 expression, as well as the PD-1 checkpoint pathway in cancer.

To further investigate the relationship between HDAC6 and key genes involved in PI3K-AKT signaling, mTOR signaling, and the Apoptosis pathway, we utilized the TIMER database. The results revealed that HDAC6 gene expression exhibited a positive correlation with the expression of genes such as PIK3CA, mTOR, AKT1, AKT2, and BCL-2, while it showed a negative correlation with the pro-apoptotic BID gene (supplementary Fig. 1E). By integrating the results of these analyses, we speculate that HDAC6 plays a pivotal role in regulating both tumor progression and the tumor immune microenvironment in LUAD.

### Modifications of HDAC6 in LUAD

An analysis of the TCGA database was carried out to identify genetic modifications of HDAC6. The frequency of different genetic modifications of HDAC6 varied among cancers, with approximately 3.53% of LUAD patients having genetic abnormalities, with the main types being "mutation" and "amplification" (supplementary Fig. 2A)[19–21]. We identified the top 20 most mutated genes in different HDAC6-expressing subgroups. High expression of HDAC6 most often occurred with mutations in the TP53 (53%), TTN (45%) and MUC16 genes (39%) (supplementary Fig. 2B), while low expression of HDAC6 often co-occurred with TTN (45%), TP53 (42%), and MUC16 (40%) mutations (supplementary Fig. 2C). Waterfall plot revealed 92.16% (235/255) somatic mutation rate in high HDAC6 expression and the low expression group had a somatic mutation rate of 92.19% (236/256) (supplementary Fig. 2B). Overall, mutations occurred slightly more frequently in the HDAC6 high-expression cohort than in the low-expression cohort; the difference was not highly significant. Regarding DNA methylation, we discovered that there was no apparent difference in the methylation level of HDAC6 between tumor and normal samples (supplementary Fig. 3D, E), indicating that the promoter methylation of

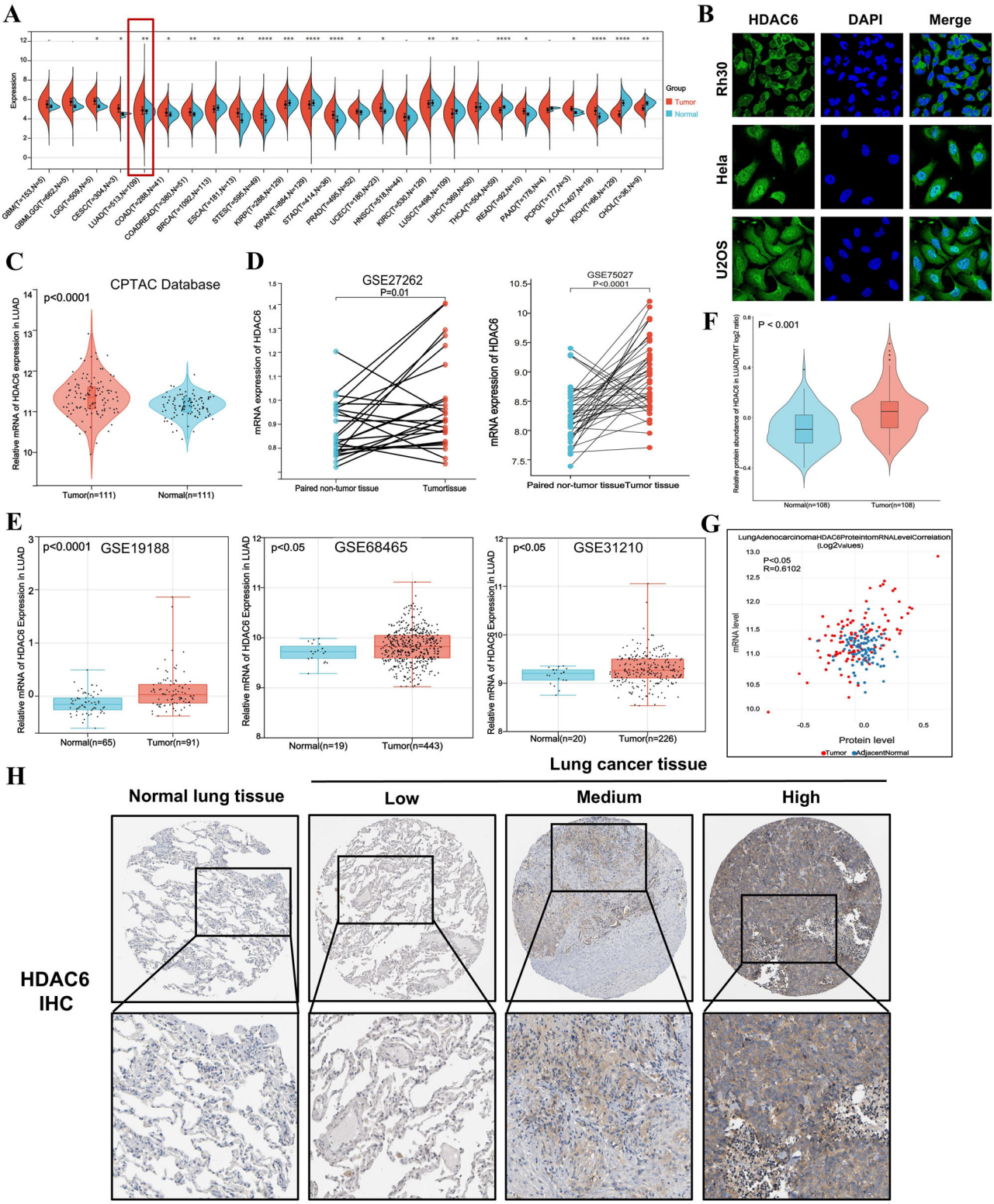


**Fig. 1 | HDAC6 expression levels in pan-cancer and LUAD. A** Expression levels of HDAC6 mRNA in pan-cancer, compared with normal tissue from the TCGA database. **B** Intracellular localization of HDAC6 in different cell lines based on HPA database. **C** The mRNA expression of HDAC6 between LUAD and normal in CPTAC database. **D** The mRNA expression of HDAC6 between LUAD and paired non-tumor tissue in GES27262 and GSE75027 datasets. **E** Expression levels of HDAC6 mRNA in LUAD and normal across three GEO datasets. **F** Protein expression of HDAC6 in LUAD samples in comparison to that in healthy tissue samples from the CPTAC database. **G** The correlation between HDAC6 mRNA and protein abundance. **H** IHC images of HDAC6 protein in LUAD obtained from HPA database.

HDAC6 may not cause changes in the mRNA level. In addition, "arm-level gain" CNVs had an inverse association with the infiltration of immune cells, including B cells, CD4 + T cells, Macrophages, Neutrophils and Dendritic cells (supplementary Fig. 3F). And, "High Amplication" CNVs also had an inverse association with the infiltration of Neutrophils and Dendritic cells (supplementary Fig. 3F).

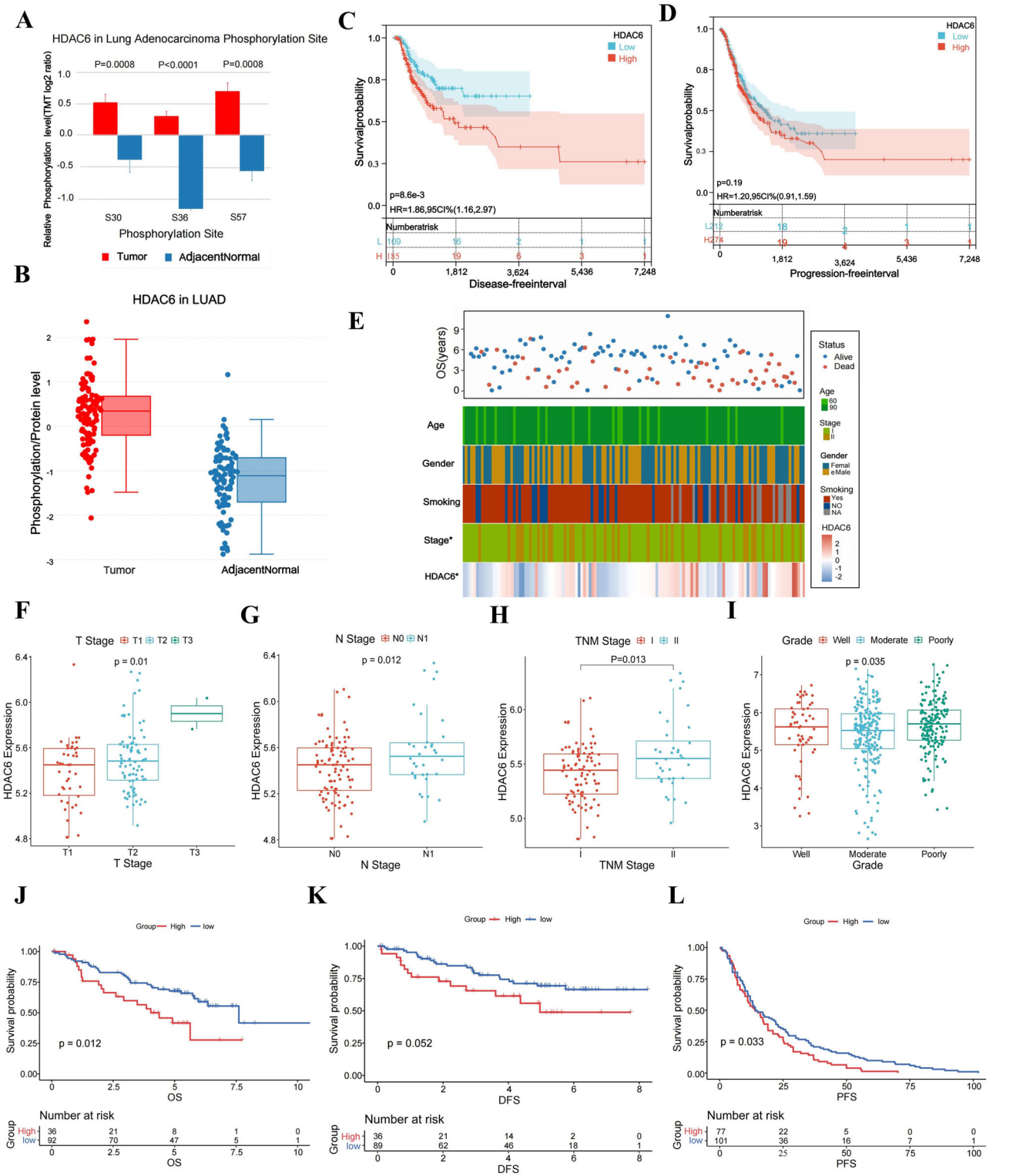


**Fig. 2 | Phosphorylation levels of HDAC6, prognostic value and associations with clinicopathological characteristics in LUAD. A** Relative phosphorylation level of different HDAC6 phosphorylation sites in LUAD samples in comparison to that in healthy tissue samples from the TCGA database. **B** Phosphorylated HDAC6 protein abundance in tumor and normal lung tissues from the TCGA database. **C**, **D** High HDAC6 expression was accompanied by worse Disease-free interval (DFI) and Progression-free interval (PFI). **E** HDAC6 relationships with clinical features of patients with LUAD based on GSE50081 data. **F–I** HDAC6 was significantly increased in LUAD samples with a high degree of malignancy, as indicated by factors such as advanced T-stage, N-stage, TNM stage (GSE50081), and poor differentiation (GSE68465). **J–L** High expression of HDAC6 in patients with LUAD was associated with poor OS (GSE50081), DFS (GSE50081), and PFS (GSE68465). $*p < 0.05$; $**p < 0.01$; $***p < 0.001$; $****p < 0.0001$.

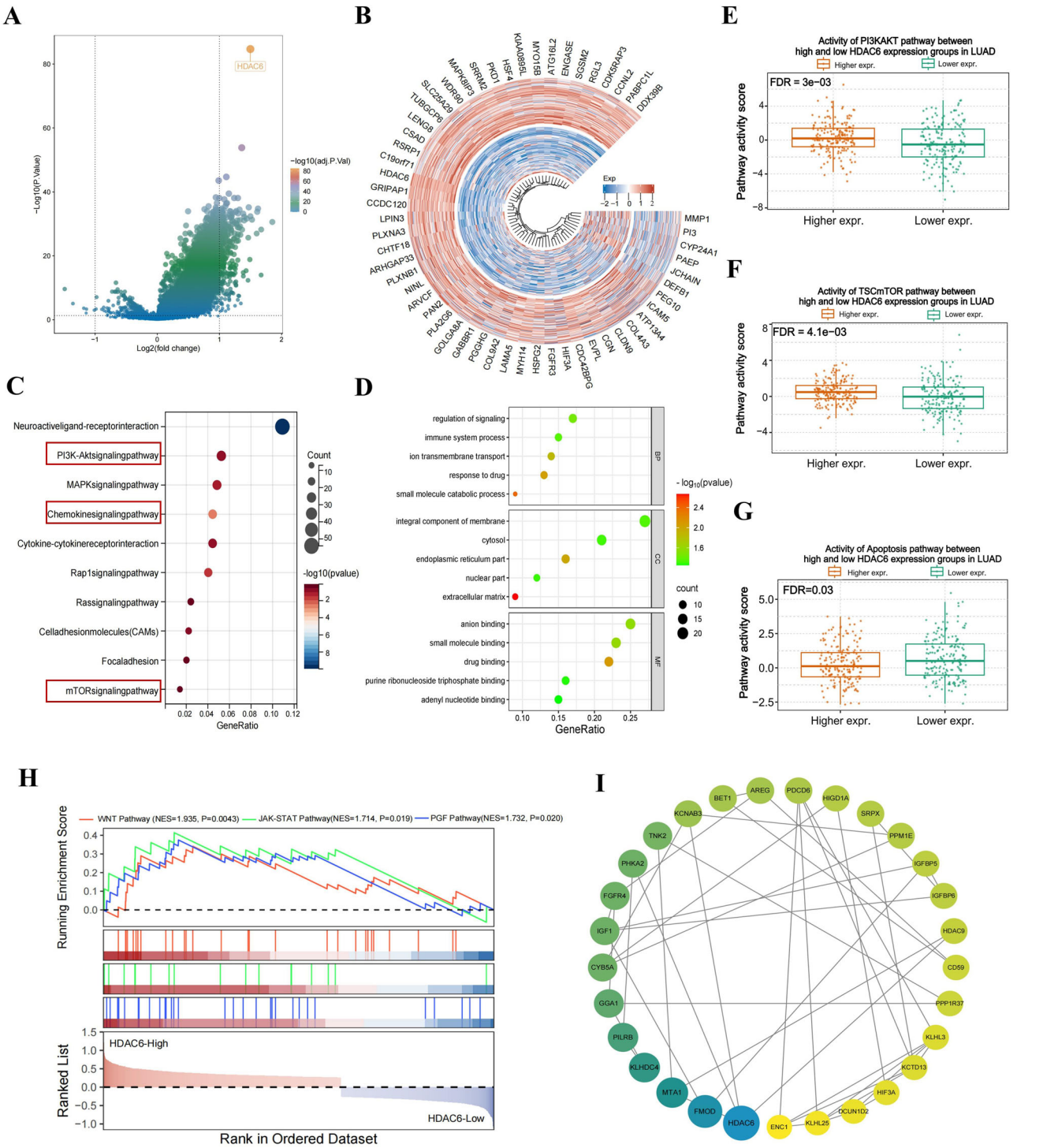


**Fig. 3 | Functional enrichment analysis of HDAC6 in LUAD based on TCGA database. A** Differential gene volcano map between high and low HDAC6 expression groups. **B** Heatmap of top differential genes between high and low HDAC6 expression groups. **C** Top 10 KEGG analysis terms of HDAC6 co-expressed genes. **D** Top 5 GO analysis terms of HDAC6 co-expressed genes, including biological process (BP), cellular component (CC), and molecular function (MF) terms. **E–G** Top 3 enriched pathways' activity of HDAC6 co-expressed genes in the TCGA database from the GSCA website. **H** Top 3 pathways of HDAC6 upregulated related genes. **I** PPI network of HDAC6 co-expressed genes.

## HDAC6 reshaped the immune microenvironment in LUAD

Immunotherapy has become an important treatment modality for LUAD[22]. Cancer immune-therapy stimulates the immune response and modulates the tumor immune microenvironment, which in turn activates T-cells to exert anti-tumor effects. In addition, T cells make up the majority of tumor-infiltrating lymphocytes and these lymphocytes are usually associated with a good prognosis and a better response to immunotherapy[23]. Our KEGG results showed that HDAC6 co-expressed genes were enriched in the T-cell receptor and chemokine receptor pathways, suggesting a possible role of HDAC6 in the immunomodulation of LUAD. Therefore, we next performed a comprehensive analysis to investigate the relationship between HDAC6 expression and tumor immune microenvironment factors,

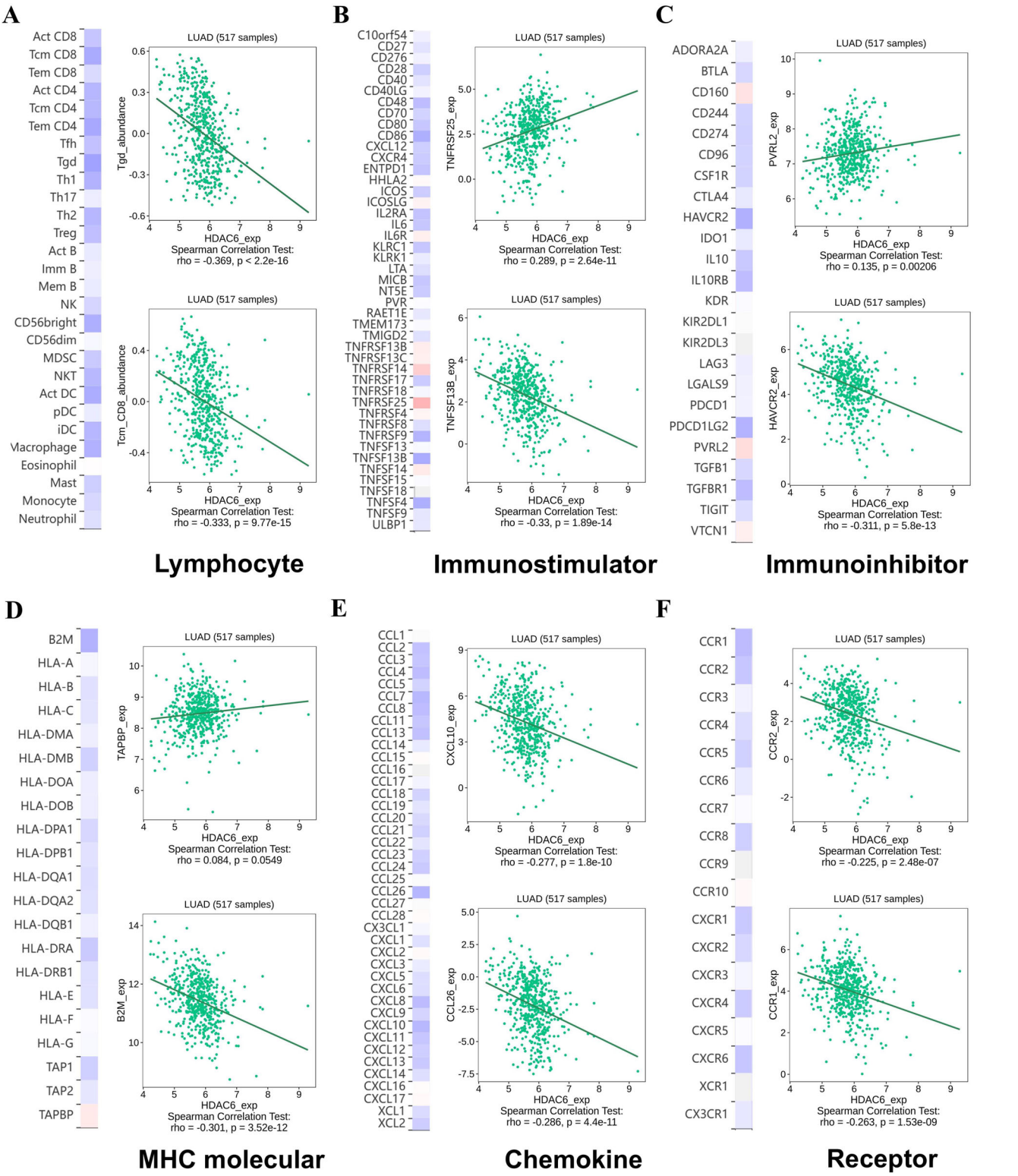


**Fig. 4 | Association of HDA6 expression with lymphocytes, immunomodulators, MHC molecules, chemokines and chemokine receptors. A–F** Correlation of HDAC6 with lymphocytes (**A**), immunostimulators (**B**), immunoinhibitors (**C**), MHC molecules (**D**), chemokines (**E**) and chemokine receptors (**F**).

including lymphocytes, checkpoints, MHC molecules, chemokines and receptors. Figure 4 showed the molecules with the highest associations: lymphocytes: Tgd cells (r = -0.369, $p < 2.2e-16$), Tcm CD8 + T cells (r = −0.333, $p < 9.77e-15$); immunostimulators: TNFRSF25 (r = 0.289, $p = 2.64e-11$) and TNFSF13B (r = -0.33, $p < 1.89e-14$); inhibitory immune molecules: PVRL2 (r = 0.135, $p = 0.00206$), HAVCR2 (r = −0.311, $p = 5.8e-13$); MHC molecules: TAPBP (r = 0.084, $p = 0.0549$), B2M (r = -0.301, $p = 3.52e-12$); chemokines: CXCL10 (r = −0.277 $p = 1.8e-10$), CCL26 (r = −0.286, $p = 4.4e-11$); and chemokine receptors: CCR2 (r = −0.225, $p = 2.48e-07$), CCR1 (r = −0.263, $p = 1.53e-09$).

Moreover, our results revealed that patients with HDAC6 high expression had relatively lower stromal score ($P = 7.87e-7$, Fig. 5A), immune score ($P = 3.2e-4$, Fig. 5B), and estimate score ($P = 5.5e-6$, Fig. 5C) compared with the low expression group. To understand the relationship between

HDAC6 and infiltrating immune cells, a correlation analysis across HDAC6 and markers for immune cells was firstly performed by GEPIA database. These biomarkers are widely used for the purpose of immune cell characterization. We analyzed the correlation between specific gene markers of different T cell subtypes, NK cells, DC cells, B cells, monocytes, MDSCs, CAFs, and the expression of HDAC6. We found that in LUAD patients with high HDAC6 expression, the specific gene markers of Tregs, exhausted T cells, MDSCs, and CAFs were significantly increased, while the specific gene markers of immune-activating cells such as B cells, CD8 + T cells, Th1 cells, NK cells, and DC cells were significantly decreased (Fig. 5D, E). Interestingly, HDAC6 expression was shown to be positively correlated with the phenotype of M2-type macrophages, such as CD206 and CD163 expression, while negatively correlated with the phenotype of M1-type macrophages, such as CD86 and CD64 expression. This implies that overexpression of HDAC6 could promote the polarization of M1-type to M2-type macrophage (Fig. 5F). Then we further proved by TIMER database that HDAC6 expression was significantly negatively correlated with infiltrating levels of B cells, CD8 + T cells, NK cells and DC, and significantly positively correlated with infiltrating levels of CD4 + T cells, macrophages, and Tregs (Fig. 5G).

To further validate the difference in immune cell infiltration between different HDAC6 expression groups, we employed the CIBERSORT algorithm on data from the TCGA database. Our analysis revealed that Tregs, monocytes, M0 macrophages, M2 macrophages, and CAFs were significantly upregulated in the cohort exhibiting high HDAC6 expression. Conversely, M1 macrophages, neutrophils, and the cytotoxicity score were significantly downregulated (Fig. 6A-C). The correlation plot in Fig. 6D further confirmed our previous findings, highlighting a particularly strong association between HDAC6 expression and B cells, CD8 + T cells and M2 macrophages. In addition, we explored the relationship between differential HDAC6 expression and inhibitory immune molecules in LUAD. Our results showed significant upregulation of IGSF8, CD160, LAG3, PRVL2, and VTCN1 in the high HDAC6 expression group (Fig. 6E). These findings were consistent with the results obtained from the GSE50081 and GSE68465 datasets (supplementary Fig. 3A-D), reinforcing the robustness of our observations. In summary, we propose that the HDAC6 gene in LUAD may reshape the TIME by promoting the differentiation and infiltration of immunosuppressive T cells (such as Tregs and exhausted T cells), while inhibiting the infiltration and function of immune-activating T cells (such as CD8 + T cells and Th1 cells), as well as B cells, NK cells, and DC cells, and by regulating macrophage polarization.

### HDAC6 could potentially predict immunotherapy response in LUAD

We conducted an analysis to investigate the correlation between HDAC6 expression and biomarkers of immunotherapy response. Our findings indicated that HDAC6 exhibited a positive association with TMB and MSI (Fig. 6F, G). This suggested that patients with high HDAC6 expression had an enhanced capacity to recruit immune cells for tumor recognition. However, no significant difference was observed in the TIDE score between the high and low HDAC6 expression groups (Fig. 6H). Furthermore, we delved deeper into the analysis by examining the differences in IPS scores among LUAD patients in the two groups. Our results revealed that IPS scores were lower in the HDAC6 high-expression group, which could possibly indicate a poorer response to immunotherapy with PD-1 and CTLA4 inhibitors and a heightened likelihood of immune escape (Fig. 6I). Taken together, our findings suggest that immunotherapy is more likely to benefit patients with low HDAC6 expression. Therefore, HDAC6 may serve as a valuable biomarker for identifying suitable candidates for immunotherapy among patients with LUAD.

### HDAC6 expression was associated with the efficacy of multiple antitumor drugs

To investigate the clinical relevance of HDAC6 expression, we examined the correlation of its expression with the IC50 values of multiple antitumor drugs (screening criteria: $P < 0.05$, $|R| > 0.20$). The IC50 values of multiple antitumor drugs were negatively correlated with the expression of HDAC6, such as ACY-1215, Apitolisib, Afatinib, Canertinib, Osimertinib, Tipifarnib and so on. We also investigated the sensitivity of the two groups to multiple targeted drugs and we found patients with high HDAC6 expression had lower IC50 values for most targeted drugs, such as Tipifarnib, Linsitinib, Afatinib, and Lapatinib, than patients with low expression, indicating that targeted therapy might have better efficacy in patients with high expression of HDAC6 (Fig. 7A, B).

### Expression and prognostic value of HDAC6 in our clinical samples

We conducted experiments using qRT-PCR and WB to validate the results obtained from the TCGA database, using both normal and LUAD cells. Our results showed that HDAC6 was upregulated in most LUAD cells at the protein and mRNA level (Fig. 8A, B). Moreover, IHC results also verified a considerably higher HDAC6 expression in LUAD samples compared to adjacent normal lung tissues ($P = 0.002$) (Fig. 8C). Typical images of different staining intensities of HDAC6 were shown in Fig. 8D. The baseline information of our clinical data showed in Table 1. Furthermore, we analyzed above clinical data, showing that LUAD patients with high HDAC6 expression ($n = 69$) had significantly poor OS ($P < 0.0001$) and DFS ($P < 0.0001$) (Fig. 8E, F).

Univariate and multivariate COX analysis revealed that HDAC6 was an independent prognostic factor for OS in LUAD patients (Fig. 9A, B). The Cox regression analyses revealed that HDAC6 score (HR = 1.01, 95%CI (1.01–1.02), $P = 1.8e-7$) was a prognostic variable independent of age, ECOG score, T stage, N stage and pTNM stage. Using the independent markers of prognosis, we constructed a nomogram to predict 1-year, 2-year and 3-year OS for LUAD patients (Fig. 9C). C-index of the model was 0.76, 95% CI (0.70-0.82), $p = 1.47e-17$. The calibration plots demonstrated that the prediction of the model was well matched with the observed 2-year and 3-year OS rates, while there was a bias in the predictive efficacy of one-year OS, possibly related to the small number of patients in this group (Fig. 9D). The ROC curves analyses showed that the AUC values based on HDAC6 IHC score, age and pTNM stage at 1-year, 2-year, and 3-year OS being 0.72 (95%CI: 0.89-0.54), 0.84 (95%CI: 0.89–0.79), and 0.80 (95%CI: 0.87–0.73), respectively (Fig. 9E). In addition, the risk score distribution, survival status, and expression levels of HDAC6 were shown in Fig. 9F. When the risk score increased, the risk of death of LUAD patients increased, while the survival time decreased (Fig. 9F).

### HDAC6 promoted the aggressiveness of LUAD cells

To further experimentally confirm the specific role of the HDAC6 gene in LUAD, we transfected lentiviruses carrying a stable knockout of HDAC6 into the A549 and H1299 cell lines. As shown in Fig. 10A, B, the knockout effect was verified at both the protein and mRNA levels, respectively. We then conducted CCK8 and clone formation assays on both wild-type and HDAC6 knockout cell lines. Our results revealed that the proliferation and clone formation abilities of the HDAC6 knockout cell lines were significantly reduced (Fig. 10C, D). Furthermore, we performed Transwell and wound healing assays on the two groups of cells. Our findings indicated that the migration and invasion abilities of LUAD cells were significantly decreased after the knockout of HDAC6 (Fig. 10E, F). These results provide further experimental evidence supporting the role of HDAC6 in LUAD progression.

By integrating data from the TCGA, GSE50081, and GSE68465 databases, we observed that the differential genes between the HDAC6 high and low expression groups were significantly enriched in the PI3K/AKT/mTOR pathway and the apoptosis pathway. We further by WB experiments compared the differences in PTEN, p-AKT, AKT, p-mTOR, and mTOR levels between the HDAC6 Vector group and the HDAC6 KO group in A549 and H1299 cell lines. We found that after HDAC6 knockout, PTEN expression levels were significantly increased, while p-AKT and p-mTOR expression were significantly decreased, indicating that the PI3K/AKT/

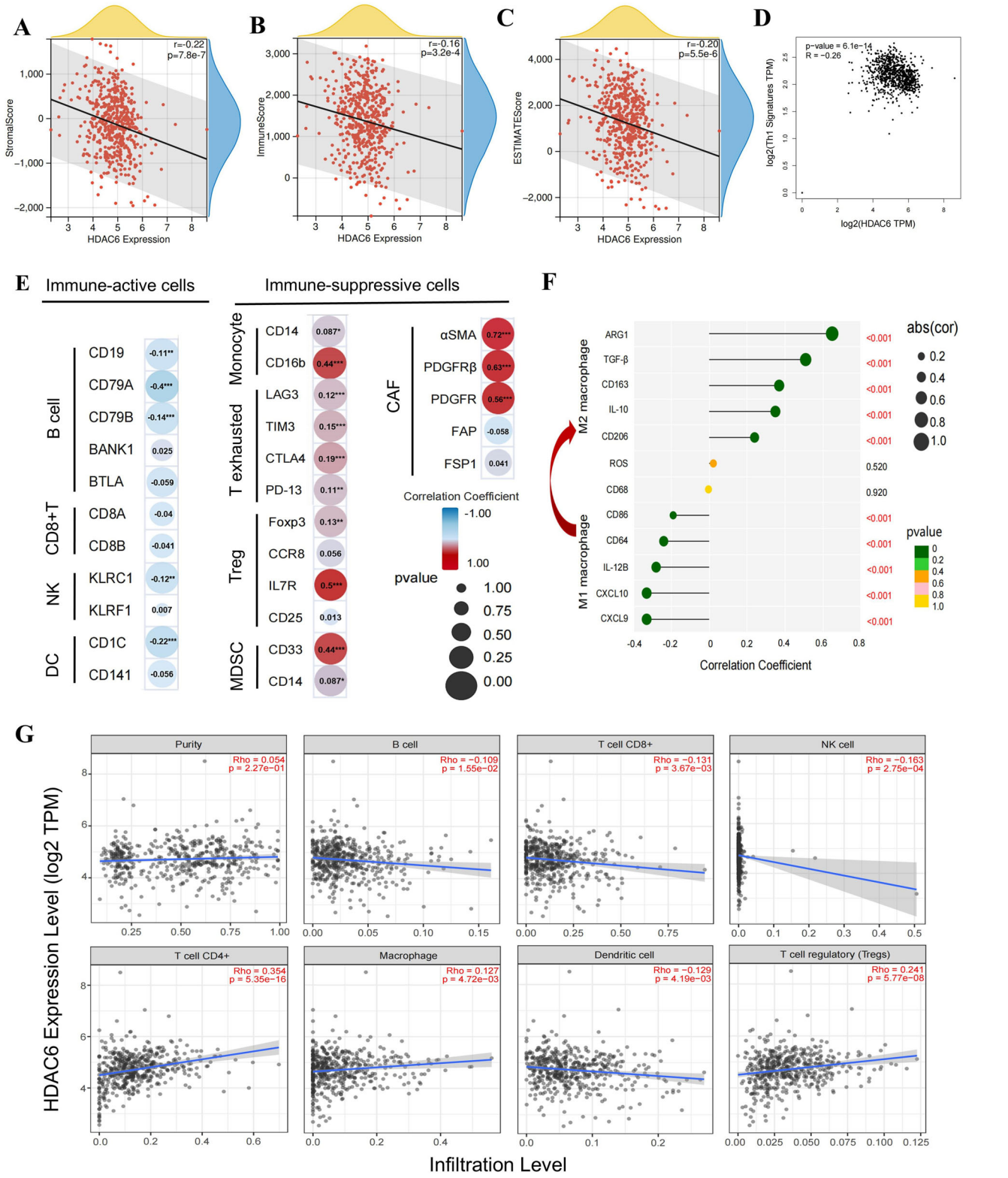


**Fig. 5 | Upregulated HDAC6 shapes an immune-suppressive tumor microenvironment based on TCGA database. A–C** Correlations between HDAC6 expression and stroma score, immune score, estimate score. **D**, **E** Correlations between HDAC6 expression and the immune cell markers. **F** HDAC6 expression correlates with macrophages polarization. **G** HDAC6 expression was significantly negatively correlated with infiltrating levels of B cells, CD8 + T cells, NK cells and DC, and significantly positively correlated with infiltrating levels of CD4 + T cells, macrophages, and Tregs. *$p < 0.05$; **$p < 0.01$; ***$p < 0.001$; ****$p < 0.0001$.

mTOR pathway was markedly inhibited (Fig. 11A, B). Notably, previous studies have demonstrated that hyperactivation of the PI3K/AKT/mTOR pathway can promote EMT[24]. Therefore, we conducted WB experiments to analyze the expression levels of key molecules related to EMT, such as E-cadherin, N-cadherin, vimentin, snail, and slug, as well as key molecules involved in the apoptotic pathway, including the anti-apoptotic gene BCL-2 and the pro-apoptotic genes Bax, Bim, and cleaved-caspase3, in both wild-type and HDAC6 knockout cell lines (Fig. 11C-F). Our results revealed that

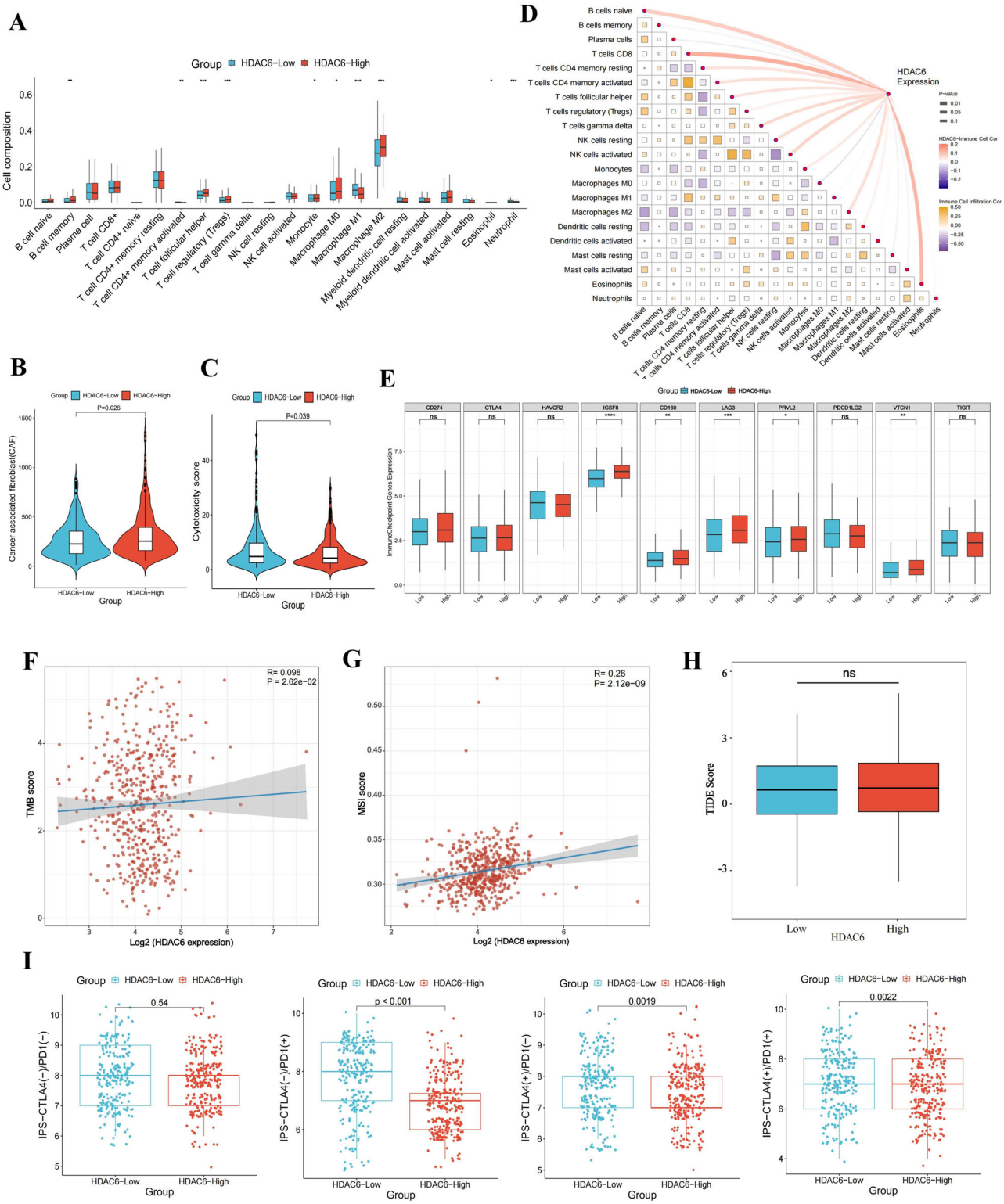


**Fig. 6 | Correlation of HDAC6 expression with immune cell infiltration, inhibitory immune molecules, and immunotherapy response in the TCGA LUAD cohort. A–C** The 22 immune cell composition (**A**), CAF (**B**) and cytotoxicity score (**C**) expression in different HDAC6 expression in LUAD patients. **D** Correlation of different immune cell infiltrations in the TCGA database and respective correlation with HDAC6 expression. **E** Immune exhaustion molecules expression in different HDAC6 expression in LUAD patients. **F–H** Correlation of immunotherapy response biomarkers, including tumor mutation burden (TMB) (**F**), Microsatellite Instability (MSI) (**G**), and tumor immune dysfunction and exclusion (TIDE) score (**H**), with HDAC6 expression in the TCGA cohort. **I** Immune cell proportion score (IPS) between the HDAC6 high and low expression groups in the TCGA cohort. $^{*}p < 0.05$; $^{**}p < 0.01$; $^{***}p < 0.001$; $^{****}p < 0.0001$.

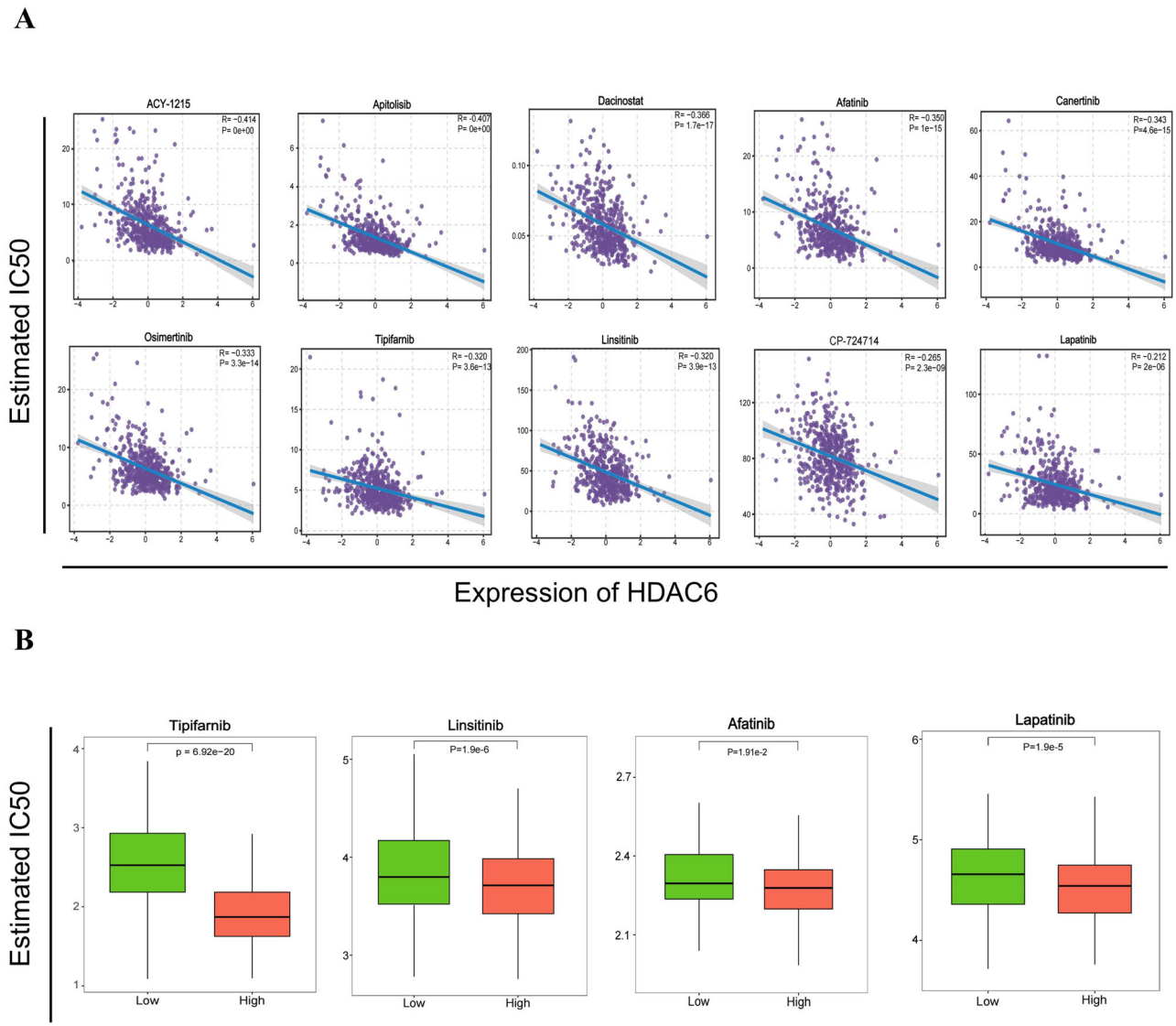


**Fig. 7 | Evaluation of drug sensitivity correlated with HDAC6 expression in LUAD. A** The comparisons in IC50 value of 10 anti-tumor drugs between the HDAC6 high and low expression groups in the TCGA cohort. **B** Correlation of HDAC6 expression with the estimated IC50 values of 4 targeted drugs in the TCGA cohort.

the EMT phenomenon was significantly suppressed, while the apoptotic pathway was activated in both A549 and H1299 cell lines after the knockout of the HDAC6 gene. These findings were further corroborated by qRT-PCR experiments (Fig. 11G).

### HDAC6 regulated macrophage polarization in LUAD TIME

Based on the results of our TCGA database analysis, we identified a crucial role for HDAC6 in regulating a diverse array of immune cells within the LUAD TIME, particularly macrophages. To further investigate this, we initially induced adherent growth of THP-1 cells (representing M0 macrophages) using PMA. Subsequently, we co-cultured these macrophages with both wild-type A549 and H1299 cell lines, as well as their HDAC6 knockout counterparts. Upon co-culturing M0 macrophages with the tumor cells, we observed morphological changes in a subset of the macrophages, transitioning from a round shape to an elongated spindle shape, indicative of macrophage polarization (Fig. 11H). To elucidate the underlying molecular changes, we extracted total mRNA from the co-cultured macrophages and conducted qRT-PCR experiments. Our results revealed that M1 macrophage-associated gene markers, such as CD86, CXCL9, and NOS2, were significantly up-regulated in macrophages co-cultured with sgHDAC6-1 LUAD cell lines. Conversely, M2 macrophage-associated gene markers, including CD206, ARG1, and IL-10, were significantly down-regulated (Fig. 11I, J). To assess the functional implications of these findings, we added conditioned media collected from wild-type and HDAC6 knockout A549 and H1299 cell lines to the lower chamber of a transwell system and observed the migration ability of macrophages in the upper chamber. Our results demonstrated that the migration ability of macrophages in the HDAC6 knockout group was significantly enhanced (Fig. 12A, B). These findings align with the results obtained from the TCGA database, suggesting that HDAC6 plays a pivotal role in regulating the polarization of M1 to M2 macrophages and inhibiting macrophage recruitment within the LUAD TIME.

### HDAC6 inhibition enhances the efficacy of anti-PD-1 therapy in LUAD

Based on the preliminary experimental results, we conducted further exploration in animal models. Firstly, we injected A549 wild-type cells and HDAC6 KO A549 cells subcutaneously into two groups of BALB/C nude mice to establish subcutaneous xenograft models. We found that the tumor weight and volume in the HDAC6 KO group were significantly lower than those in the control group, while there was no significant difference in body weight or growth between the two groups (Fig. 12C–F). In summary, based on our cellular experiments, animal experiments, and clinical sample data from our institution, we propose

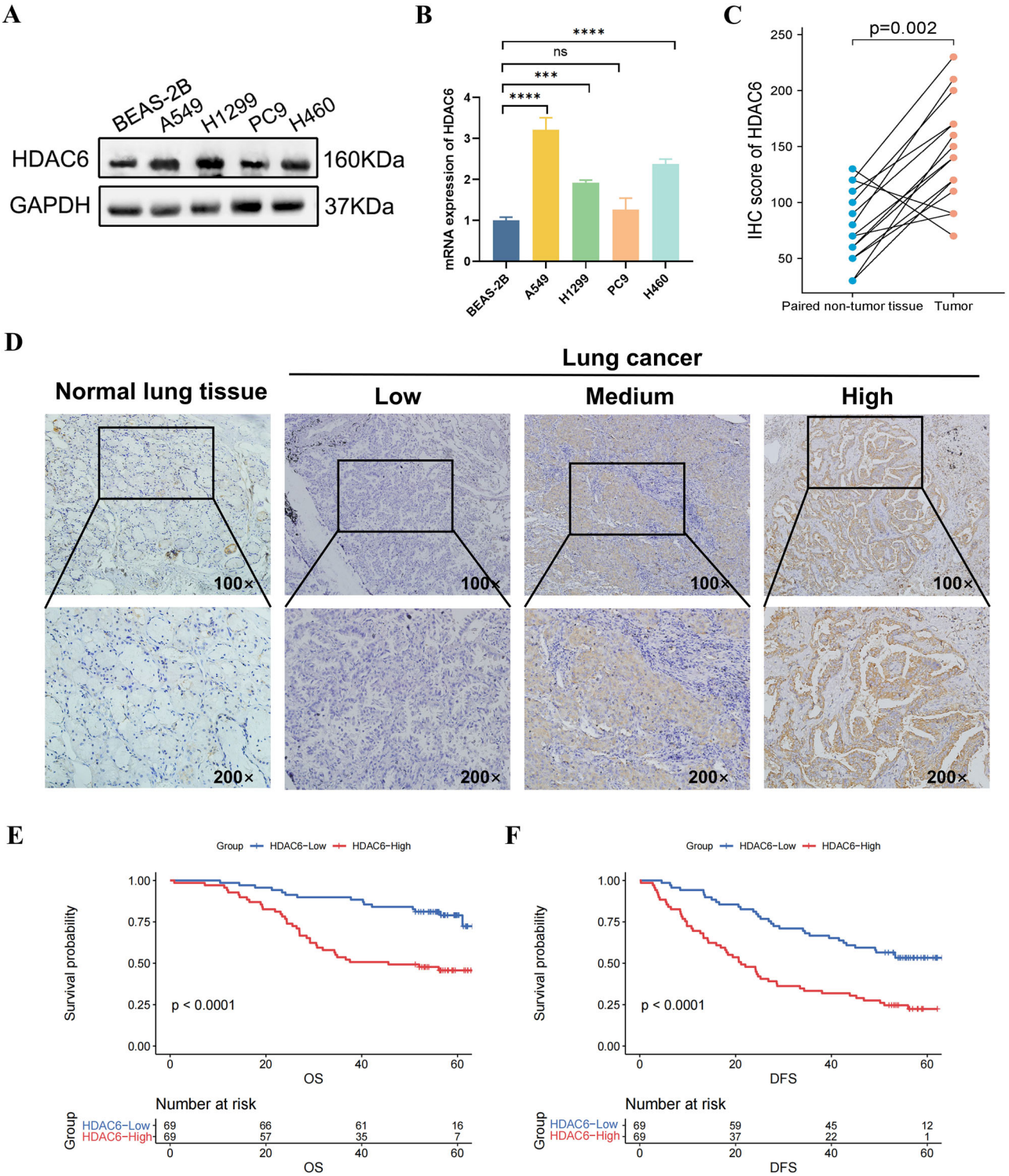


**Fig. 8 | Expression and clinical value of HDAC6 in our clinical samples. A**, **B** The protein and mRNA level of HDAC6 in different LUAD and normal lung cell lines. **C** The differential expression of HDAC6 in paired non-tumor tissues ($n = 15$) and LUAD tissues ($n = 15$). **D** The typical IHC staining images of HDAC6 in normal lung tissues and LUAD tissues. **E**, **F** The KM curves about the correlation between HDAC6 expression and OS (**E**) and DFS (**F**). $^{*}p < 0.05$; $^{**}p < 0.01$; $^{***}p < 0.001$; $^{****}p < 0.0001$.

that HDAC6 can serve as a prognostic marker for LUAD patients, with high HDAC6 expression potentially indicating a worse prognosis. In addition, based on our findings that HDAC6 may play an important role in reshaping the TIME in LUAD, we have conducted preliminary explorations in preclinical models. We injected LLC cells subcutaneously into C57BL/6 mice and divided them into four groups: a control group, an HDAC6 inhibitor monotherapy group (Tubastatin A), a PD-1 inhibitor monotherapy group, and a combination therapy group. We found that the combination therapy group exhibited significantly stronger tumor growth inhibition compared to the monotherapy groups, suggesting that HDAC6 inhibitors can synergize with PD-1 inhibitors to exert anti-tumor effects in LUAD (Fig. 12G–J).

**Table 1 | Clinical characteristics of 138 patients with LUAD**

| Characteristics | Total N = 138 (%) | HDAC6-Low N = 69 (%) | HDAC6-High N = 69 (%) | P |
|---|---|---|---|---|
| Age | | | | 0.62 |
| Mean ± SD | 59.12 ± 9.05 | 59.97 ± 9.24 | 58.28 ± 8.84 | |
| Median (min-max) | 59 (31,79) | 60 (31,79) | 59 (31,78) | |
| Gender | | | | 0.50 |
| Female | 73 (52.90%) | 39 (56.52%) | 34 (49.28%) | |
| Male | 65 (47.10%) | 30 (43.48%) | 35 (50.72%) | |
| Smoking history | | | | 0.39 |
| NO | 78 (56.52%) | 42 (60.87%) | 36 (52.17%) | |
| YES | 60 (43.48%) | 27 (39.13%) | 33 (47.83%) | |
| ECOG | | | | 0.73 |
| 0 | 61 (44.20%) | 32 (46.38%) | 29 (42.03%) | |
| 1 | 77 (55.80%) | 37 (53.62%) | 40 (57.97%) | |
| T-Stage | | | | 0.73 |
| I | 79 (57.25%) | 42 (60.87%) | 37 (53.57%) | |
| II | 54 (39.13%) | 24 (34.78%) | 30 (26.79%) | |
| III | 3 (2.17%) | 2 (2.90%) | 1 (12.5%) | |
| IV | 2 (1.45%) | 1 (1.40%) | 1 (7.14%) | |
| N-Stage | | | | 0.28 |
| 0 | 69 (50.00%) | 35 (50.72%) | 34 (49.28%) | |
| 1 | 11 (7.97%) | 3 (4.35%) | 8 (11.59%) | |
| 2 | 58 (42.03%) | 31 (44.93%) | 27 (39.13%) | |
| M-Stage | | | | 1.00 |
| 0 | 138 (100%) | 69 (100%) | 69 (100%) | |
| pTNM-Stage | | | | 0.22 |
| I | 65 (47.10%) | 33 (47.83%) | 32 (46.38%) | |
| II | 14 (10.14%) | 4 (5.80%) | 10 (14.49%) | |
| III | 59 (42.75%) | 32 (46.38%) | 27 (39.13%) | |
| Progress Status | | | | <0.001 |
| NO | 53 (38.41%) | 37 (53.62%) | 16 (23.19%) | |
| YES | 85 (61.59%) | 32 (46.38%) | 53 (76.81%) | |
| OS Status | | | | <0.001 |
| Dead | 52 (37.68%) | 15 (52.38%) | 37 (25.00%) | |
| Live | 86 (62.32%) | 54 (47.62%) | 32 (75.00%) | |

*ECOG* Eastern Cooperative Oncology Group performance, *SD* standard deviation, *OS* overall survival.

There was no significant difference in body weight among the four groups of mice (Fig. 12K).

## Discussion

Histone deacetylases are a family of enzymes that play important roles in epigenetic and transcriptional regulation[25]. In recent years, numerous pan-HDAC inhibitors and HDAC6-selective inhibitors have undergone clinical trials across various tumor types[26,27]. Notably, a clinical trial revealed promising activity when combining HDAC and mTOR inhibition in patients with relapsed or refractory Hodgkin lymphoma[28]. Furthermore, a phase I study demonstrated that the HDAC inhibitor panobinostat, in conjunction with intensive induction chemotherapy, achieved a complete response rate of 32% in older patients with acute myeloid leukemia[29]. A multicenter phase Ib clinical trial also showed that the HDAC6 inhibitor ricolinostat, in combination with lenalidomide and dexamethasone, achieved an overall response rate of 55% in patients with relapsed or refractory multiple myeloma[30]. Currently, clinical trials focusing on inhibitors of the HDAC family, particularly those targeting HDAC6, are predominantly conducted in hematological tumors. However, given the epigenetic properties of the HDAC6 target and its widespread high expression across multiple tumor types, there remains considerable potential to explore HDAC6 inhibitors that are efficacious against solid tumors, including LUAD.

Our study found that HDAC6 was upregulated in multiple cancer types including LUAD, compared to normal tissues. HDAC6 tended to be enriched in tumors with a higher degree of malignancy, as indicated by factors such as more advanced TNM stage and poor differentiation. Both from public databases and experimental validation, our results showed that LUAD patients with high HDAC6 expression had a poorer prognosis and it was an independent prognostic factor for LUAD patients. In clinical practice, we could attempt to achieve precise stratification of LUAD patients by detecting HDAC6 expression levels in tumor tissues, helping to identify high-risk patient groups and thereby guiding the formulation of individualized treatment strategies. In terms of treatment selection, HDAC6 inhibitors may enhance the efficacy of immunotherapy by modulating the tumor microenvironment (e.g., promoting M1 macrophage polarization and inhibiting Treg infiltration), particularly when combined with PD-1/

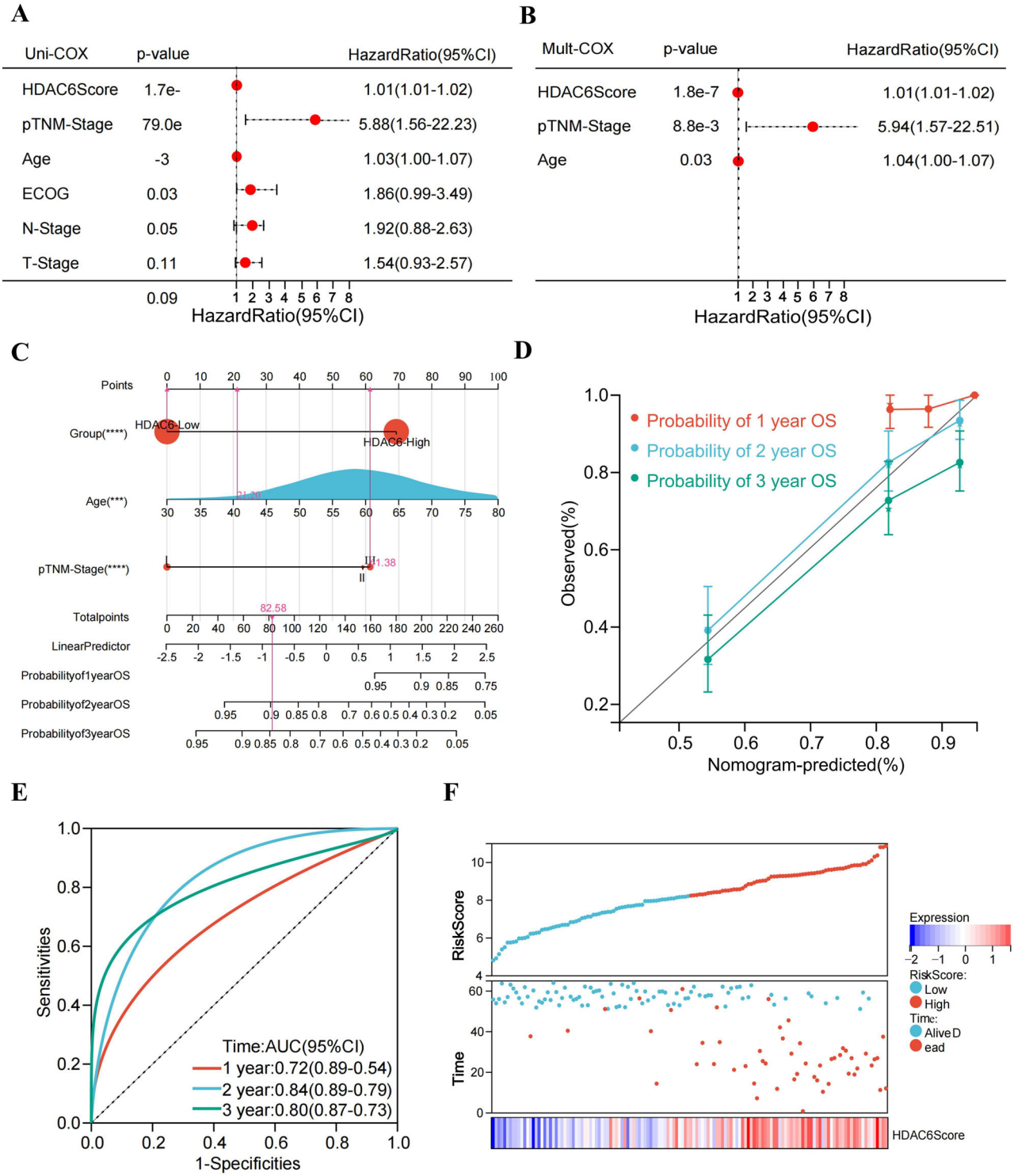


**Fig. 9 | HDAC6 can independently predict the OS of patients with LUAD. A**, **B** Univariate and multivariate COX analyses for OS. **C**–**E** The nomogram, calibration curves and ROC curves for OS based on HDAC6 IHC score, age and TNM stage. **F** Distribution of risk score, survival status, and the expression of HDAC6.

PD-L1 inhibitors, potentially reversing the immunosuppressive microenvironment and improving treatment response rates. Meanwhile, some studies had shown that HDAC6 was highly expressed in tumors such as colorectal cancer[31] and melanoma[32], which was often accompanied by both poorer OS and suppressive TIME. The above results suggested that HDAC6 functioned as an oncogene in a variety of tumors.

In addition, it was interesting to note that we found that LUAD patients had a higher frequency of somatic mutations, especially TP53, TNN and MUC16 gene, implying more instability of the genome and more production of tumor neoantigens than those with low expression of HDAC6[33]. We found that DNA mutation and amplification of HDAC6 were rare in LUAD (approximately 3.53%). Furthermore, DNA methylation of HDAC6 had little influence on its mRNA expression. The analysis showed that HDAC6 negatively regulated the infiltration of multiple immune cells, including B cells, CD4 + T cells, Macrophages, Neutrophils and Dendritic cells mainly through "arm-level gain" and "High Amplication"CNVs.

Functionally, HDAC6 distinguishes itself from other HDAC proteins by primarily localizing to the cytoplasm and possessing the unique ability to

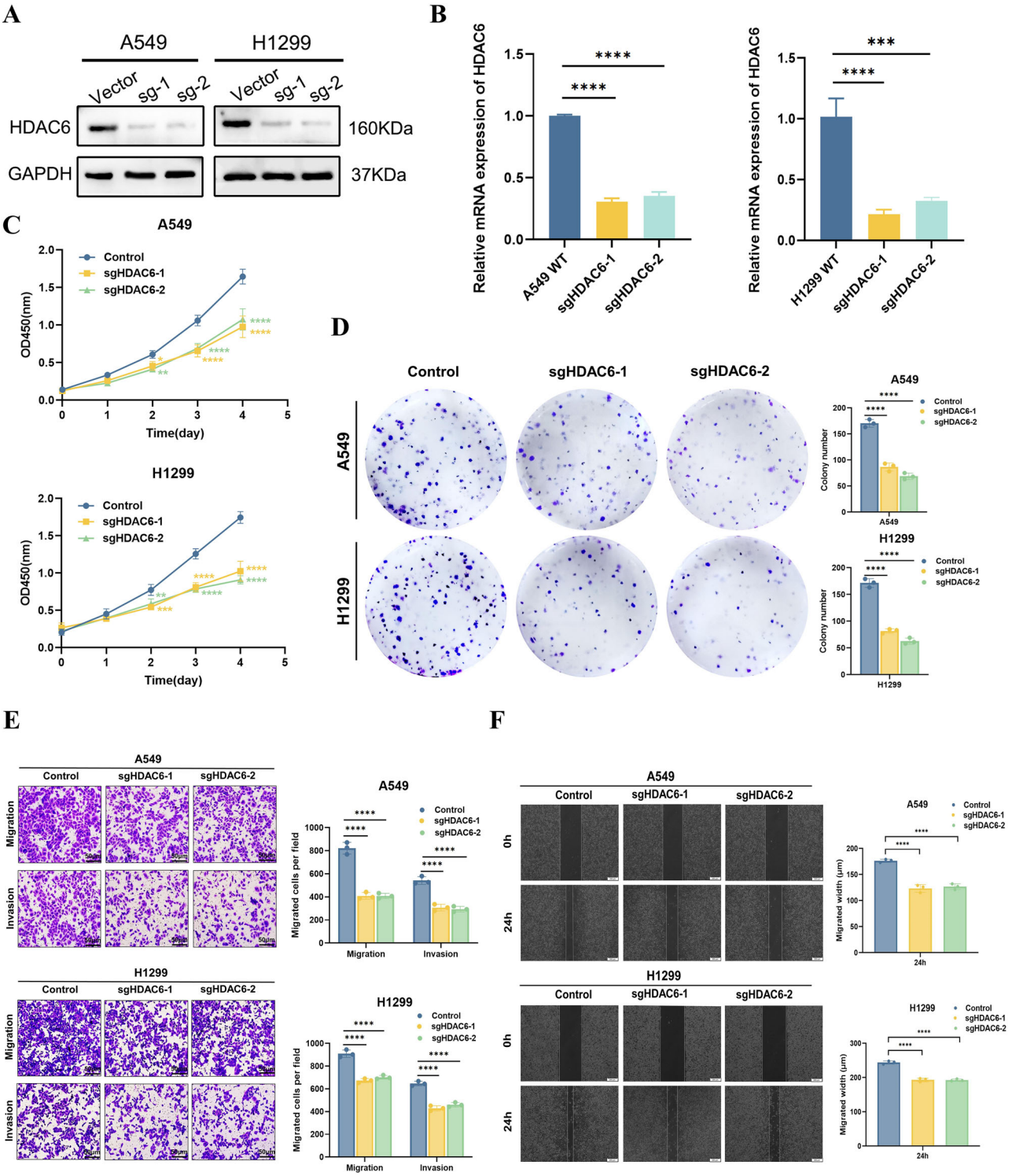


**Fig. 10 | HDAC6 promoted the aggressiveness of LUAD cells. A**, **B** WB and qRT-PCR validated HDAC6 knockdown efficiency at protein and mRNA levels, respectively. **C**, **F** CCK8 assay (**C**), clone formation assay (**D**), Transwell assay (**E**) and wound healing assay (**F**) between A549 and H1299 wild cell lines and knockout HDAC6 cell lines. *$p < 0.05$; **$p < 0.01$; ***$p < 0.001$; ****$p < 0.0001$.

deacetylate a diverse array of nonhistone proteins[34]. Research has demonstrated that HDAC6 can regulate the deacetylation status of its substrate HSP90, thereby modulating the activity of the PI3K/AKT pathway and further influencing the proliferation of tumor cells[10]. Our findings align with this perspective.

By analyzing data from the database, we discovered that the differentially expressed genes between the high and low HDAC6 expression groups were enriched in the PI3K/AKT signaling pathway, mTOR signaling pathway, and apoptosis pathway. Furthermore, our experimental validation confirmed that HDAC6 knockout promoted apoptosis and significantly inhibited the proliferation, migration, invasion, and EMT transformation of LUAD cells. However, the precise regulatory mechanism of HDAC6 in LUAD remains to be further elucidated through sequencing techniques such as RNA-seq, CUT&TAG, and ATAC-seq.

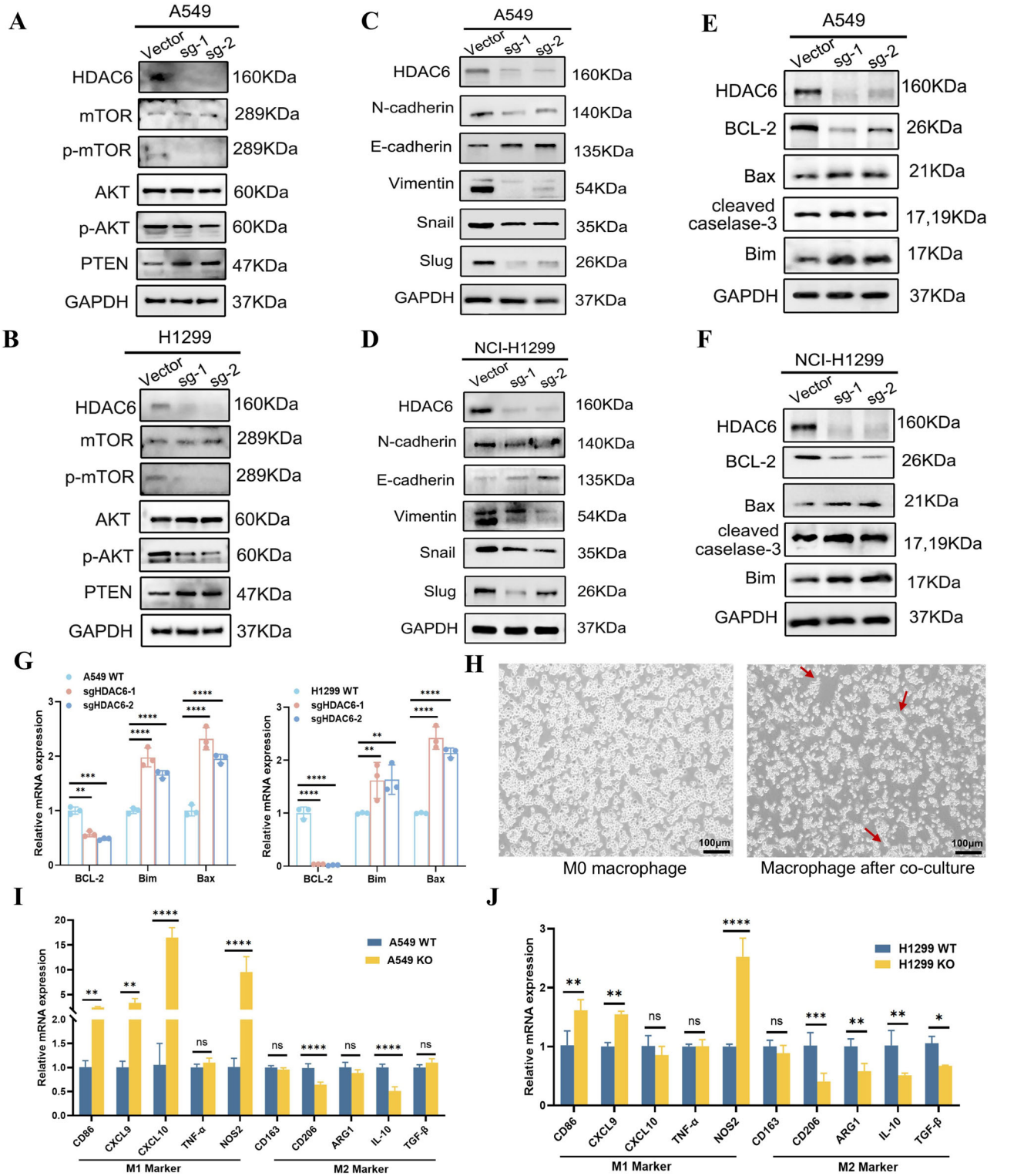


**Fig. 11 | HDAC6 regulated PI3K/AKT/mTOR, EMT, apoptosis and macrophage polarization in LUAD cells. A**, **B** WB experiments of PI3K/AKT/mTOR-related key molecules and apoptotic pathway-related key molecules in wild cell lines and knockout HDAC6 cell lines. **C**–**F** WB experiments of EMT-related key molecules and apoptotic pathway-related key molecules in wild cell lines and knockout HDAC6 cell lines. **G** qRT-PCR validation of apoptosis pathway-related molecules. **H** M0 macrophage morphology and macrophage morphology after co-culture with tumor cells. **I**, **J** Effect of the HDAC6 gene on macrophage polarization in the LUAD cell line. $^{*}p < 0.05$; $^{**}p < 0.01$; $^{***}p < 0.001$; $^{****}p < 0.0001$.

HDAC6 has been implicated in regulating not only tumor proliferation and invasion but also the tumor immune microenvironment[35]. Specifically, it promotes an anti-inflammatory phenotype in tumor-associated macrophages (TAMs), while HDAC6 inhibition enhances the pro-inflammatory TME and antitumor immune response in colon cancer[36], breast cancer[37] and melanoma cancer[38]. Consistently, our study indicates that HDAC6 may regulate the TME in LUAD. High HDAC6 expression in LUAD was associated with an immunosuppressive TME, characterized by low immune

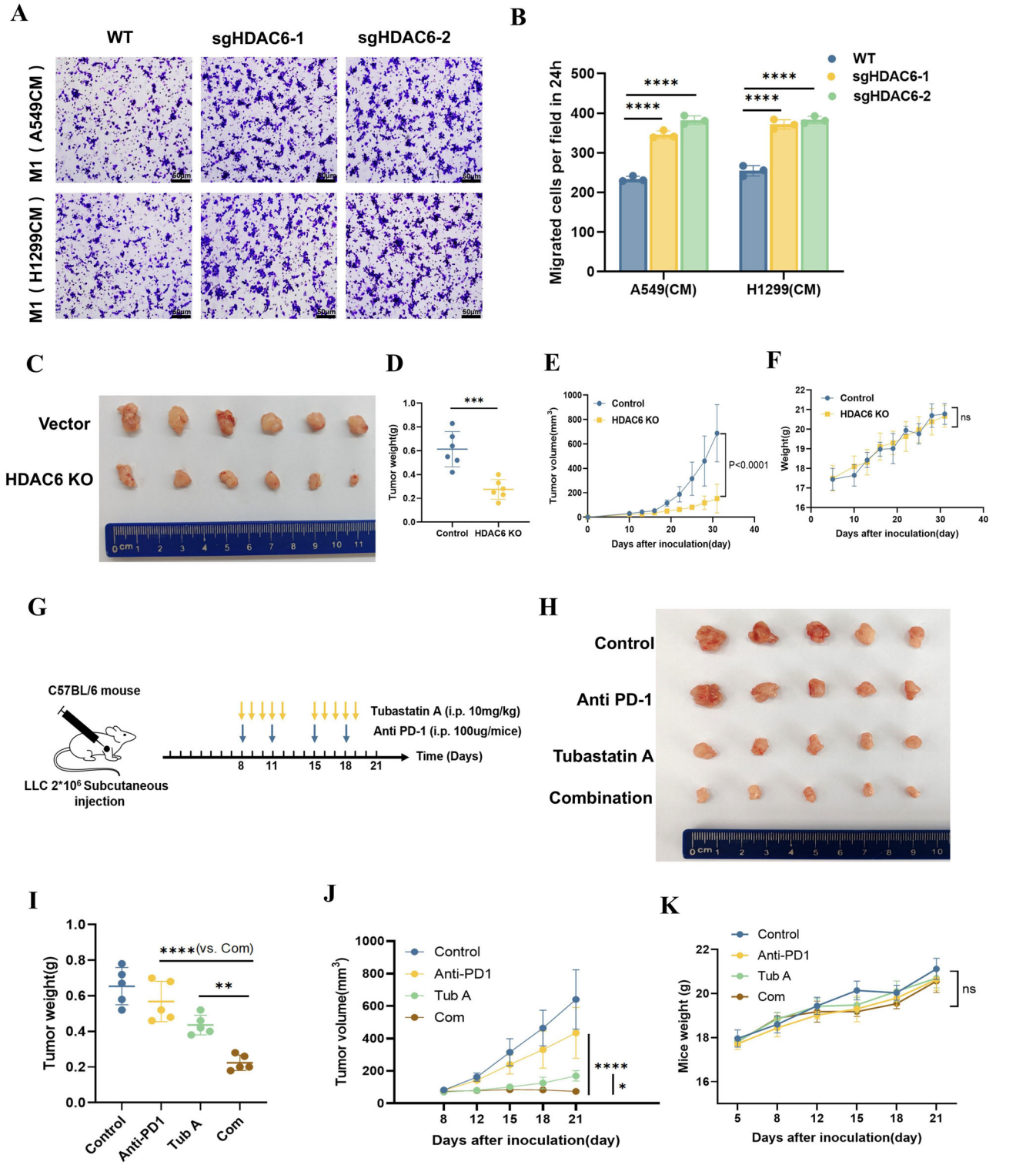


**Fig. 12 | HDAC6 inhibition could enhance the efficacy of anti-PD-1 therapy in lung adenocarcinoma.** **A**, **B** Effect of HDAC6 gene on macrophage migration in LUAD cell line. CM: Conditioned Medium (**C**) BALB/C nude mice were implanted with 5 × 106 HDAC6 KO or control A549 cells. **D**, **E** Comparison of tumor weight and volume between two groups. **F** The body weight measurements of mouse were taken every 3 days. **G**, **H** C57BL/6 mice were implanted with $2 \times 10^6$ LLC cells and subsequently treated with either the PD-1 monoclonal antibody alone, the HDAC6 inhibitor Tubastatin A alone, or a combination of both drugs. **I**, **J** Comparison of tumor weight and volume among different groups. **K** The body weight measurements of mice were taken every 3 days. $^*p < 0.05$; $^{**}p < 0.01$; $^{***}p < 0.001$; $^{****}p < 0.0001$.

scores, reduced infiltration of B cells and CD8 + T cells, and increased infiltration of suppressive immune cells like CAFs and MDSCs. In terms of mechanisms: our preliminary bioinformatics analysis results (Fig. 4E) showed that the expression of HDAC6 was significantly negatively correlated with the expression of chemokines such as CXCL9, CXCL10, and CCL2. Additionally, the co-culture results of tumor cells and macrophages (Fig. 11E, F) demonstrated that after HDAC6 knockout, the expression of chemokines such as CXCL9 and CXCL10 was significantly increased, and

**Table 2 | Clinical characteristics of patients with LUAD from multiple cohorts**

| Characteristics | TCGA N = 492 (%) | GSE68465 N = 439 (%) | GSE50081 N = 128 (%) |
|---|---|---|---|
| Age | | | |
| Median | 66 | 65 | 70.15 |
| Range | 33-88 | 33-87 | 40.16-85.91 |
| Gender | | | |
| Female | 264 (53.66) | 218 (49.66) | 63 (49.22) |
| Male | 228 (46.34) | 221 (50.34) | 65 (50.78) |
| Smoking history | | | |
| Yes | 407 (82.72) | 299 (68.11) | 92 (71.88) |
| NO | 71 (14.43) | 48 (10.93) | 23 (17.97) |
| NA | 14 (2.85) | 92 (20.96) | 13 (10.15) |
| TNM Stage | | | |
| I | 266 (54.07) | 275 (62.64) | 92 (71.88) |
| II | 120 (24.39) | 96 (21.87) | 36 (28.12) |
| III | 80 (12.26) | 68 (15.49) | / |
| IV | 26 (5.28) | / | / |
| OS Status | | | |
| Dead | 179 (36.38) | 234 (53.30) | 52 (40.63) |
| Live | 313 (63.62) | 205 (46.70) | 76 (59.37) |

*NA* not available, *OS* overall survival.

the recruitment of macrophages in the tumor immune microenvironment was also markedly enhanced. Therefore, based on the results of HDAC6's association with the infiltration and differentiation of different immune cells, we hypothesized that HDAC6 may reduce the infiltration of CD8 + T cells and NK cells by suppressing the expression of CXCL9 and CXCL10, while promoting the secretion of CCL2 to increase the recruitment of Tregs and MDSCs. However, the aforementioned hypotheses still require experimental validation.

Although high TMB and MSI scores are predictive of good responses to immune checkpoint inhibitors (ICIs) in melanoma and NSCLC[39]. Interestingly, we found that LUAD patients with high HDAC6 expression had higher TMB and MSI score but poorer predicted response to CTLA4 or PD1 treatment, which implied that HDAC6 might have caused immune escape from LUAD, but the exact mechanism needed to be further verified. In addition, reduction of M2 macrophage polarization by pharmacological HDAC6 inhibition has recently been described[34]. In line with this, our findings revealed that HDAC6 regulates M1-type macrophage to M2-type macrophage polarization in LUAD, and knockout of HDAC6 significantly increased M1-type macrophage recruitment in LUAD tumor microenvironment. High expression of HDAC6 in LUAD was associated with poor prognosis. We considered that not only a result of tumor cell proliferation enhanced by HDAC6 but also a result of antitumor TME suppression.

Although few clinical trials of HDAC6 inhibitor monotherapy have been conducted in solid tumors, it still has the potential to work synergistically with chemotherapeutic agents, targeted agents, and immunological agents. A previous study revealed that coupling the immune-modulatory properties of the HDAC6 inhibitor ACY241 with Oxaliplatin could promote robust anti-tumor response in NSCLC[35]. Moreover, a study found that combining DNMT and HDAC6 inhibitors increased anti-tumor immune signaling and decreased tumor burden in ovarian cancer[40]. In our study, we found that LUAD patients with high HDAC6 expression may be more sensitive to drugs such as ACY-1215, Apitolisib, Afatinib, Canertinib, Osimertinib and so on. These drugs were in part HDAC6 inhibitors, PI3K/AKT/mTOR pathway inhibitors, and EGFR inhibitors, which was consistent with the results of the HDAC6-related pathways discussed in the previous section. Therefore, targeting HDAC6 in LUAD can be considered in combination with the above drugs.

In conclusion, HDAC6 played a crucial role in promoting LUAD malignancy and reshaping its TIME via a complex mechanism. It induced EMT, enhancing LUAD cell aggressiveness, and regulated immune cell infiltration, particularly M2 macrophage polarization. This altered the tumor's immune landscape, impacting progression and treatment responsiveness. Thus, HDAC6 maybe emerged as a key prognostic marker for LUAD, providing insights into disease biology and therapeutic targets.

## Methods

### Samples and cell lines

HDAC6 gene expression and corresponding clinical data were downloaded from TCGA database (https://portal.gdc.cancer.gov/). Moreover, two independent cohorts from GEO datasets (https://www.ncbi.nlm.nih.gov/) were used for validation: GSE50081 ($n = 128$) and GSE68465 ($n = 439$). Only patients with complete follow-up and tumor stage information were enrolled. Table 2 shows the baseline clinical characteristics of patients with LUAD in the TCGA and GEO datasets. In addition, the datasets GSE27262, GSE75027, GSE19188, and GSE31210 mentioned in the article were also obtained from the GEO database. Cell lines used in this study, including BEAS-2B, A549, NCI-H1299, PC9, NCI-H460, LLC and THP-1 cells were provided by American Type Culture Collection (ATCC) cell bank.

### Expression landscape and prognostic value of HDAC6 gene

We utilized multiple bioinformatic databases to investigate the expression and prognostic value of HDAC6 in LUAD. The differential expression of HDAC6 in pan-cancerous tissues and normal tissues was examined using the Sangerbox Online Website Platform (http://vip.sangerbox.com/home.html)[41]. The correlation between HDAC6 mRNA expression and protein expression was analyzed by the cProSite database (https://cprosite.ccr.cancer.gov/) and protein expression differences of HDAC6 in LUAD and normal tissue were accessed via the CPTAC database (https://hupo.org/Clinical-Proteome-Tumor-Analysis-Consortium(CPTAC)). The Intracellular localization of HDAC6 in different cell lines and immunohistochemical staining on microarrays of LUAD patients and normal lung tissues were obtained from the HPA database (https://www.proteinatlas.org/). Correlations between HDAC6 expression and clinicopathological features in LUAD patients were analyzed using the ANOVA or Wilcoxon test followed by visualization through the "ggplot2" package.

### Functional enrichment analysis

Genes related to HDAC6 were identified by Pearson correlation analysis using the TCGA and two GSE datasets. Differentially expressed genes in LUAD patients with low and high HDAC6 expression were screened using the "limma" package, applying a screening criterion of $|Log2FC| > 2$ and $P < 0.05$. Meanwhile, Kyoto Encyclopedia of Genes and Genomes (KEGG) analysis and the Gene Set Enrichment Analysis (GSEA) were used to identify enriched pathways. And the gene ontology (GO) analysis was performed to validate the role of HDAC6 in LUAD. These functional enrichment results were derived from the R package "ClusterProfiler". The top three KEGG-enriched pathways enriched for HDAC6 co-expressed genes were obtained from the GSCA database (https://guolab.wchscu.cn/GSCA/#/)[42]. Additionally, protein-protein interaction (PPI) analysis was performed to identify co-expressed genes of HDAC6, using a correlation index greater than 0.4 as the criterion, and the PPI networks was generated from the STRING database (https://cn.string-db.org/). The most correlated subnetworks were identified using the Mcode plugin of Cytoscape and their biological functions were visualized through the Cluego plugin.

### Gene alteration analysis

cBioPortal (https://www.cbioportal.org/) was used to identify modifications of the HDAC6 gene across cancers, and specifically in LUAD, based on

TCGA data. Mutation waterfall plots of the high and low HDAC6 expression groups were identified by the "maftools" package. The DNMIVD (http://www.unimd.org/dnmivd/) database was used to compare the methylation level of HDAC6 between tumor and normal samples. The association between CNVs of HDAC6 and immune cell infiltration was analyzed by the TIMER (https://cistrome.shinyapps.io/timer/) database.

### Immune infiltration analysis and immunotherapeutic response prediction

We analyzed the correlation between HDA6 expression and immune microenvironment factors through TISIDB (http://cis.hku.hk/TISIDB/index.php), including lymphocytes, immunostimulators, immunoinhibitors, MHC molecules, chemokines and chemokine receptors, which is an integrated database for tumor-immune system interactions. In addition, the "ESTIMATE" package was utilized to calculate the estimate score, immunity score, and stroma score for every LUAD sample. We further analyzed the correlation between HDAC6 expression and immune cell-specific markers by the GEPIA2.0 database ((http://gepia.cancer-pku.cn/). The association between HDAC6 expression and immune cell infiltration was analyzed by the TIMER (https://cistrome.shinyapps.io/timer/) database. The online web tool CIBERSORT (https://cibersort.stanford.edu/) was employed to determine the immune cell infiltration levels of each sample by uploading the gene expression matrix of LUAD. A Wilcoxon test was then employed to assess the correlation between HDAC6 and immune checkpoints by comparing low and high HDAC6 expression groups. To evaluate the differentiation between tumor immune dysfunction and exclusion (TIDE) scores, we uploaded the normalized gene expression matrix to the TIDE website (http://tide.dfci.harvard.edu) and the Wilcoxon test was utilized to compare the estimates of different HDAC6 expression groups. Tumor mutational burden (TMB) value and Microsatellite instability (MSI) were calculated for each LUAD patient using the "maftools" package. In addition, we downloaded the Immune cell proportion score (IPS) scores of LUAD patients via the TCIA database (https://tcia.at/home) and further analyzed the differences in scores between high and low HDAC6 expression groups.

### Drug sensitivity analysis

The chemotherapeutic response of TCGA patients was evaluated based on drug sensitivity data from the Genomics of Drug Sensitivity in Cancer (GDSC) database (https://www.cancerrxgene.org/). The half-maximal inhibitory concentrations (IC50) values of antitumor drugs were estimated using the "pRRophetic" package, which utilized the gene expression matrix from individual LUAD patient. Comparative analysis of drug sensitivity was performed on the high and low HDAC6 expression groups. Additionally, the correlation coefficient was calculated by the Spearman correlation test between drug sensitivity and HDAC6 expression (from the BEST website: https://rookieutopia.hiplot.com.cn/app_direct/BEST/).

### Cell culture and construction of stably infected cell lines

The human NSCLC cell lines (A549, NCI-H1299, PC9, NCI-H460) and BEAS-2B cell were cultured in RPMI 1640 medium (Gibco, USA) with 10% fetal bovine serum (Zeta Life, France) and penicillin-streptomycin solution (50 μg/mL). LLC cells were cultured in DMEM medium (Gibco, USA), with all other conditions being the same as for other cells. THP-1 cells were cultured in RPMI 1640 medium supplemented with an additional 0.05 mM 2-mercaptoethanol. All cultures were maintained at 37 °C under humidified atmosphere containing 5% CO2.

Stable cell lines (A549-HDAC6-sg1, A549-HDAC6-sg2, H1299-HDAC6-sg1, H1299-HDAC6-sg2) were generated using lentiviral transduction. Lentivirus was generated in 293 T cells by transfecting the transfer plasmid (HDAC6-sgRNA series) together with packaging plasmids PLP1, PLP2 and VSVG. Briefly, sgRNA sequences targeting promoters of HDAC6 (see Supplementary Table 1) were cloned into lentiCRISPRv2. Target cells were transfected with lentiviral particles followed by Puromycin selection (2 μg/mL).

### Western blotting (WB)

The protein extraction and western blotting processes were performed as described in our previous publication[43]. The primary antibodies were listed below: GAPDH (1:1000 dilution, CST Cat#3700), HDAC6 (1:1000 dilution, Proteintech Cat#12834-1-AP), mTOR (1:1000 dilution, CST Cat#2983), p-mTOR (Ser2448) (1:1000 dilution, CST Cat#5536), AKT (1:1000 dilution, CST Cat#4691), p-AKT (Ser473) (1:2000 dilution, CST Cat#4060), PTEN (1:1000 dilution, CST Cat#9559), N-cadherin (1:1000 dilution, CST Cat#13166), E-cadherin (1:1000 dilution, CST Cat#3195), Vimentin(1:1000 dilution, CST Cat#5741), Snail (1:1000 dilution, CST Cat#3879), Slug (1:1000 dilution, CST Cat#9585), Bcl2 (1:1000 dilution, CST Cat#2764), Bax (1:1000 dilution, CST Cat#2772), Bim(1:1000 dilution, CST Cat#2933), Cleaved-casepase3 (1:1000 dilution, CST Cat#9664). Western blot stripping buffer (P0025) was purchased from Beyotime Biotechnology (Shanghai, China). Note: To detect protein expression on the same membrane, under the premise of ensuring the integrity of the target proteins, we hybridized with two different antibodies successively on the same blotting membrane, using the stripping buffer in the process.

### Gene expression analysis by real-time quantitative PCR (qRT-PCR)

The total RNA was extracted using the Trizol reagent following the product protocol (Invitrogen, No.15596026) and reverse transcribed total RNA into complementary DNA using PrimeScript™ RT reagent Kit (#RR420A, Takara, China). Subsequently, Universal Blue qPCR SYBR green Master Mix (Yeasen, China) was used for RT-qPCR. Primers used to analyze mRNA levels were listed in Supplementary Table 2.

### Immunohistochemistry (IHC)

In our clinical dataset, 138 LUAD samples that underwent surgery between November 2022 and January 2024 were obtained from Tianjin Cancer Institute and Hospital, which was approved by the ethics committee of the Tianjin Medical University Cancer Institute and Hospital (Ek2021098) and adhered to the ethical guidelines of the Helsinki Declaration. All patients provided written consent for the use of their specimens and data. Termination time of follow-up of our clinical data was May 20, 2024. The detailed IHC procedures was followed by our previous study[43]. Antigen retrieval was performed with pressure cooking in tris-EDTA (pH = 9.0). We used antibody against HDAC6 (Proteintech Cat#12834-1-AP) at a dilution of 1:200.

### Prognostic analysis

The Kaplan-Meier (KM) analysis was conducted based on the survival time in the low and high group of HDAC6 expression (training set and validation set). Univariate and multivariate Cox regression analysis were performed to examine the correlation between survival time, clinical prognostic indicators and HDAC6 expression using the "survival" package. Nomograms were constructed based on the independent factors of Cox multivariate analyses by "rms" package. The concordance index (C-index) and calibration were assessed to effectively measure the performance of constructed nomograms. The "SurvivalROC" package was applied to generate receiver operating characteristic (ROC) curves to assess predictive performance.

### Cell proliferation

A549 and H1299 cells infected with control lentivirus and HDAC6-knockout lentivirus were seeded into 96-well plates at a density of 2000 cells per well. At 24, 48, 72 h, 96 h after the cells were seeded, CCK-8 reagent (Zeta, France) was mixed with the cells for 2 h incubation at 37 °C in the dark. The absorbance value was measured at 450 nm with Microplate reader.

Additionally, the plate colony formation assay was performed to evaluate the colony formation ability of tumor cells. The stably transfected cells were seeded in six-well plates, which was assessed with crystal violet staining after 14 days cell culture.

### Transwell assay

The transwell assay for cell migration or invasion was conducted using a 24-well culture insert. 3 × 104 cells were suspended in 200 µl of serum-free RPMI-1640 media. The cell suspension was added to the upper chamber of the transwell insert, which was coated with or without a matrix component like Matrigel (BD Biosciences, NJ, USA) for invasion or migration assays. 500 µl of RPMI-1640 supplemented with 20% FBS was added to the lower chamber of the insert as a chemoattractant. The transwell chambers were incubated for 24 h to allow cells to migrate or invade through the porous membrane. After the incubation period, cells that did not migrate or invade through the membrane and remained on the upper surface of the chamber were carefully cleaned by gently wiping the surface with a cotton swab. The cells that passed through the membrane and reached the lower surface of the chamber were fixed in 4% paraformaldehyde (Solarbio, Beijing, China) and stained with crystal violet.

### Wound healing assay

The cells were seeded into six-well plates until cells confluence was 90%. The wound was induced by scraping the cell monolayer with a 100 µl pipette tip and left for 24 h before photographing.

### Cell co-culture

To establish a coculture system for macrophages and NSCLC cells in vitro, a 24 mm Transwell chamber with an 8µm pore polycarbonate membrane (Corning, USA) was used. THP-1 monocytes ($1 \times 10^6$/well) were first induced to differentiate into M0 macrophages with 150 nM PMA (Sigma, USA) in the lower chamber. A549 and H1299 cells ($5 \times 10^5$/well) were added to the upper chamber and co-cultured with M0 macrophages for 48 h. Total RNA was extracted from the cells in the lower chamber of each group, and the expression of typical M1 markers, such as CD86, and typical M2 markers, such as CD206, were detected by qRT-PCR.

### Macrophage migration assay

Firstly, conditioned media from different treatment groups of A549 and H1299 cells need to be collected and placed in the lower chamber. 5 × 104 THP-1 cells/200ul were placed into the upper chamber after PMA induced cell adherent growth. The rest of the steps were the same as Transwell assay. The difference in macrophage migration between the groups was observed after 24 h.

### In vivo tumor xenograft assays

A549 wild-type cells and HDAC6 KO A549 cells ($5 \times 10^6$ /mouse in 0.1 mL with 50% Matrigel and 50% saline) were subcutaneously injected into the groins of 6-week-old female BALB/c nude mice (purchased from Jiangsu Gempharmatech, 6 mice/group). The body weight and tumor size of the mice were measured every three days, and the tumor burden in the two groups of mice was observed after one month.

C57BL/6 mice were purchased from Jiangsu Gempharmatech (Jiangsu, China). For subcutaneous xenograft experiments, $2 \times 10^6$ LLC cells were resuspended in 100 µL PBS and injected subcutaneously into the mice. Mice which bear tumor (average size > 100 $mm^3$) were randomly separated into four groups (5 mice/group) and treated with either vehicle control or Tubastatin A alone (MCE, 10 mg/kg, i.p., five times a week for two consecutive weeks.), mouse PD-1 monoclonal antibody (mAb) (BioXcell, BE0146; New Haven, CT, USA) alone (100ug per mouse in 100 µL D-PBS buffer, i.p., twice a week, for two consecutive weeks), or their combination. The body weight and tumor size of the mice were measured every three days, and the tumor burden in the two groups of mice was observed after three weeks. The animal experiment was conducted under an approved from the Animal Care and Use Committee of Tianjin Cancer Institute & Hospital of Tianjin Medical University.

### Statistics analysis

R software (version 4.2.2) and GraphPad Prism 9 were utilized for conducting statistical analyses. Statistical significance was assigned to results with p-values less than 0.05 (ns, $p \geq 0.05$; *, $p < 0.05$; **, $p < 0.01$; ***, $p < 0.001$). For continuous variables, the association was evaluated using either the independent samples t-test (assuming normal distribution) or the Mann-Whitney U test (for skewed data). For categorical variables, the chi-square ($X^2$) test or Fisher's exact test was employed to analyze the relationship.

## Data availability

All data supporting the findings of this study are presented in the article and the Supplementary Materials. Our study does not generate any new datasets. The datasets presented in this study can be found from the following links: TCGA (https://portal.gdc.cancer.gov/), GSE50081, GSE68465, GSE27262, GSE75027, GSE19188 and GSE31210. All other raw data are available upon reasonable request from the corresponding author.

## Code availability

The code used for analysis can be accessed by the corresponding author on reasonable request.

Received: 31 December 2024; Accepted: 14 May 2025;
Published online: 22 May 2025

## References

1. Ducellier, S. et al. Dual molecule targeting HDAC6 leads to intratumoral CD4+ cytotoxic lymphocytes recruitment through MHC-II upregulation on lung cancer cells. *J. Immunother. Cancer* **12**, https://doi.org/10.1136/jitc-2023-007588 (2024).
2. Du, Q. et al. Prognostic and immunological characteristics of CDK1 in lung adenocarcinoma: a systematic analysis. *Front. Oncol.* **13**, 1128443 (2023).
3. Wattanathamsan, O. et al. Inhibition of histone deacetylase 6 destabilizes ERK phosphorylation and suppresses cancer proliferation via modulation of the tubulin acetylation-GRP78 interaction. *J. Biomed. Sci.* **30**, 4 (2023).
4. Havel, J. J., Chowell, D. & Chan, T. A. The evolving landscape of biomarkers for checkpoint inhibitor immunotherapy. *Nat. Rev. Cancer* **19**, 133–150 (2019).
5. Siegel, R. L., Miller, K. D. & Jemal, A. Cancer statistics, 2019. *Cancer J. Clin.* **69**, 7–34 (2019).
6. Jha, S. et al. Design, synthesis, and biological evaluation of HDAC6 inhibitors targeting L1 loop and serine 531 residue. *Eur. J. Med. Chem.* **265**, 116057 (2024).
7. Li, Y. & Seto, E. HDACs and HDAC inhibitors in cancer development and therapy. *Cold Spring Harbor Perspect. Med.* **6**, https://doi.org/10.1101/cshperspect.a026831 (2016).
8. Yeon, M., Kim, Y., Jung, H. S. & Jeoung, D. Histone deacetylase inhibitors to overcome resistance to targeted and immuno therapy in metastatic melanoma. *Front. Cell Dev. Biol.* **8**, 486 (2020).
9. Liang, T. et al. Design, synthesis and biological evaluation of 3, 4-disubstituted-imidazolidine-2, 5-dione derivatives as HDAC6 selective inhibitors. *Eur. J. Med. Chem.* **221**, 113526 (2021).
10. Kaur, S., Rajoria, P. & Chopra, M. HDAC6: A unique HDAC family member as a cancer target. *Cell. Oncol.***45**, 779–829 (2022).
11. Balmik, A. A., Chidambaram, H., Dangi, A., Marelli, U. K. & Chinnathambi, S. HDAC6 ZnF UBP as the modifier of tau structure and function. *Biochemistry* **59**, 4546–4562 (2020).
12. Deskin, B. et al. Inhibition of HDAC6 attenuates tumor growth of non-small cell lung cancer. *Transl. Oncol.* **13**, 135–145 (2020).
13. Li, C. et al. The immunohistochemical expression and potential prognostic value of HDAC6 and AR in invasive breast cancer. *Hum. Pathol.* **75**, 16–25 (2018).
14. Zhang, Z., Cao, Y., Zhao, W., Guo, L. & Liu, W. HDAC6 serves as a biomarker for the prognosis of patients with renal cell carcinoma. *Cancer Biomark. Sect. A Dis. markers* **19**, 169–175 (2017).

15. Zheng, Y. et al. HDAC6, modulated by miR-206, promotes endometrial cancer progression through the PTEN/AKT/mTOR pathway. *Sci. Rep.* **10**, 3576 (2020).
16. Wang, Y., Ha, M., Li, M., Zhang, L. & Chen, Y. Histone deacetylase 6-mediated downregulation of TMEM100 expedites the development and progression of non-small cell lung cancer. *Hum. Ccell* **35**, 271–285 (2022).
17. Tien, S. C. & Chang, Z. F. Oncogenic Shp2 disturbs microtubule regulation to cause HDAC6-dependent ERK hyperactivation. *Oncogene* **33**, 2938–2946 (2014).
18. Hu, C. et al. The USP10-HDAC6 axis confers cisplatin resistance in non-small cell lung cancer lacking wild-type p53. *Cell Death Dis.* **11**, 328 (2020).
19. Cerami, E. et al. The cBio cancer genomics portal: an open platform for exploring multidimensional cancer genomics data. *Cancer Discov.* **2**, 401–404 (2012).
20. de Bruijn, I. et al. Analysis and visualization of longitudinal genomic and clinical data from the AACR project GENIE biopharma collaborative in cBioPortal. *Cancer Res.* **83**, 3861–3867 (2023).
21. Gao, J. et al. Integrative analysis of complex cancer genomics and clinical profiles using the cBioPortal. *Sci. Signal* **6**, pl1. https://doi.org/10.1126/scisignal.2004088 (2013).
22. Topalian, S. L. et al. Safety, activity, and immune correlates of anti-PD-1 antibody in cancer. *N. Engl. J. Med.* **366**, 2443–2454 (2012).
23. Patil, N. S. et al. Intratumoral plasma cells predict outcomes to PD-L1 blockade in non-small cell lung cancer. *Cancer Cell* **40**, 289–300.e284 (2022).
24. Guo, L. et al. RRM2 is a putative biomarker and promotes bladder cancer progression via PI3K/AKT/mTOR pathway. *J. Cell. Physiol.* e31501. https://doi.org/10.1002/jcp.31501 (2024).
25. Tsimberidou, A. M. et al. Preclinical development and first-in-human study of KA2507, a selective and potent inhibitor of histone deacetylase 6, for patients with refractory solid tumors. *Clin. Cancer Res. Off. J. Am. Assoc. Cancer Res.* **27**, 3584–3594 (2021).
26. Horwitz, S. M. et al. Duvelisib plus romidepsin in relapsed/refractory T cell lymphomas: a phase 1b/2a trial. *Nat. Med.* **30**, 2517–2527 (2024).
27. Wang, F. et al. Combined anti-PD-1, HDAC inhibitor and anti-VEGF for MSS/pMMR colorectal cancer: a randomized phase 2 trial. *Nat. Med.* **30**, 1035–1043 (2024).
28. Janku, F. et al. Safety and efficacy of vorinostat plus sirolimus or everolimus in patients with relapsed refractory Hodgkin lymphoma. *Clin. Cancer Res. Off. J. Am. Assoc. Cancer Res.* **26**, 5579–5587 (2020).
29. Wieduwilt, M. J. et al. Histone deacetylase inhibition with panobinostat combined with intensive induction chemotherapy in older patients with acute myeloid leukemia: phase I study results. *Clin. Cancer Res. Off. J. Am. Assoc. Cancer Res.* **25**, 4917–4923 (2019).
30. Yee, A. J. et al. Ricolinostat plus lenalidomide, and dexamethasone in relapsed or refractory multiple myeloma: a multicentre phase 1b trial. *Lancet Oncol.* **17**, 1569–1578 (2016).
31. Deng, Y. et al. HDAC6-dependent deacetylation of AKAP12 dictates its ubiquitination and promotes colon cancer metastasis. *Cancer Lett.* **549**, 215911 (2022).
32. Woan, K. V. et al. Targeting histone deacetylase 6 mediates a dual anti-melanoma effect: Enhanced antitumor immunity and impaired cell proliferation. *Mol. Oncol.* **9**, 1447–1457 (2015).
33. Liang, H. et al. Characterization of somatic mutations that affect neoantigens in non-small cell lung cancer. *Front. Immunol.* **12**, 749461 (2021).
34. Kovalovsky, D. et al. The HDAC6 inhibitor AVS100 (SS208) induces a pro-inflammatory tumor microenvironment and potentiates immunotherapy. *Sci. Adv.* **10**, eadp3687 (2024).
35. Bag, A. et al. Coupling the immunomodulatory properties of the HDAC6 inhibitor ACY241 with oxaliplatin promotes robust anti-tumor response in non-small cell lung cancer. *Oncoimmunology* **11**, 2042065 (2022).
36. Xu, G. et al. HDAC6-dependent deacetylation of TAK1 enhances sIL-6R release to promote macrophage M2 polarization in colon cancer. *Cell Death Dis.* **13**, 888 (2022).
37. Banik, D. et al. HDAC6 plays a noncanonical role in the regulation of antitumor immune responses, dissemination, and invasiveness of breast cancer. *Cancer Res.* **80**, 3649–3662 (2020).
38. Knox, T. et al. Author correction: selective HDAC6 inhibitors improve anti-PD-1 immune checkpoint blockade therapy by decreasing the anti-inflammatory phenotype of macrophages and down-regulation of immunosuppressive proteins in tumor cells. *Sci. Rep.* **9**, 14824 (2019).
39. Di Mauro, A. et al. High tumor mutational burden assessed through next-generation sequencing predicts favorable survival in microsatellite stable metastatic colon cancer patients. *J. Transl. Med.* **22**, 1107 (2024).
40. Moufarrij, S. et al. Author correction: combining DNMT and HDAC6 inhibitors increases anti-tumor immune signaling and decreases tumor burden in ovarian cancer. *Sci. Rep.* **11**, 24423 (2021).
41. Shen, W. et al. Sangerbox: a comprehensive, interaction-friendly clinical bioinformatics analysis platform. *iMeta* **1**, e36 (2022).
42. Liu, C. J. et al. GSCA: an integrated platform for gene set cancer analysis at genomic, pharmacogenomic and immunogenomic levels. *Brief. Bioinform.* **24**, https://doi.org/10.1093/bib/bbac558 (2023).
43. Liu, W., Jiang, Y., Li, G., Huang, D. & Qin, T. Oxidative phosphorylation related gene COA6 is a novel indicator for the prognosis and immune response in lung adenocarcinoma. *Sci. Rep.* **14**, 25970 (2024).

## Acknowledgements

This work was supported in part by grants from National Natural Science Foundation of China [Grant No.82172635, Grant No.82272686, and Grant No.82203628], Natural Science Foundation of Tianjin [Grant No.23JCZDJC00200 and Grant No.21JCYBJC01000], Tianjin Key Medical Discipline (Specialty) Construction Project [Grant No. TJYXZDXK-010A].

## Author contributions

Y.J., J.Z. and J.Y.: investigation, methodology, validation, original draft preparation, bioinformatics analysis, editing, and revision of the manuscript. W.L., Q.D., W.L., Q.X., X.L. and H.L.: bioinformatics analysis. D.H. and T.Q.: Supervision, design, editing, and revision of the manuscript. All authors have approved the final version of this manuscript.

## Competing interests

The authors declare no competing interests.

## Additional information

**Supplementary information** The online version contains supplementary material available at https://doi.org/10.1038/s41698-025-00949-y.

**Correspondence** and requests for materials should be addressed to Dingzhi Huang or Tingting Qin.